Chem Soc Rev

TUTORIAL REVIEW

View Article Online
View Journal | View Issue

Cite this: *Chem. Soc. Rev.*, 2025, **54**, 10856

Recent progress towards catalytic asymmetric construction of inherently chiral scaffolds

Kai Zhu,[a] David R. Spring,*[b] Bing-Feng Shi*[c] and Fengzhi Zhang*[d]

Received 24th June 2025

DOI: 10.1039/d5cs00235d

rsc.li/chem-soc-rev

Inherently chiral scaffolds are a unique type of structurally fascinating building blocks, which have found increasing applications in the field of material chemistry, medicinal chemistry, asymmetric synthesis, molecular recognition and assembly. Owing to the steady demand for these chiral entities, numerous efforts have been made on their enantioselective synthesis. Among the plethora of accomplishments reported, the catalytic asymmetric strategy is emerging as one of the most efficient and sustainable approaches. This protocol provides a powerful platform to achieve enantiomerically pure inherently chiral architectures with structural diversity. In this review article, we aim to generalize the booming and remarkable advancements in asymmetric synthesis of inherently chiral calix[*n*]arenes, pillar[*n*]arenes, saddle-shaped scaffolds, mechanically interlocked molecules, and prism-like cages under catalyst control, which would offer valuable insights for future research on the rational design of conceptually novel and streamlined asymmetric synthetic systems, thereby expanding the scope/chemical space and improving the added value of inherently chiral molecules.

Key learning points

(1) The definition of inherent chirality and its distinction from classical stereogenic elements.
(2) The key factors influencing the configurational stability of inherently chiral scaffolds.
(3) Recent advancements in catalytic asymmetric synthesis of inherently chiral scaffolds.
(4) The reaction mechanism and how enantiocontrol is achieved in catalytic asymmetric processes.
(5) The utility and promising applications of inherently chiral molecules.

1. Introduction

Inherent chirality is a manifestation of molecular chirality that arises when the stereogenic unit is the entire molecular scaffold itself, rather than localized stereogenic elements (centers, axes, or planes), and it represents a compelling frontier in modern stereochemistry. Building upon the foundational principles of chirality established by Kurt Mislow and others,[1–4] Böhmer and colleagues introduced the term "inherent chirality" in 1994 to characterize calixarenes that exhibit no symmetry elements except for a C_1 asymmetry axis, thereby expanding the theoretical framework of stereochemistry.[5] To provide a rigorous theoretical basis, Schiaffino and Mandolini established the first scientific definition in 2004, characterizing inherent chirality as arising from "the introduction of curvature into an ideal planar structure that is devoid of symmetry axes in its two-dimensional representation".[6] This definition was later refined by Szumna in 2010, replacing "devoid of symmetry axes" with "devoid of perpendicular symmetry planes".[7] According to this criterion, calix[*n*]arenes,[8–11] pillar[*n*]arenes,[12–15] rigid saddle-shaped scaffolds,[16,17] mechanically interlocked molecules,[18–20] and prism-like cages[21–23] are capable of displaying this form of molecular chirality (Fig. 1).

At present, these stereogenic units are widely employed in enantioselective molecular recognition and assembly and serve as essential building blocks in functional materials, exerting a substantial impact on the development of asymmetric synthesis and material chemistry. For instance, chiral calixarenes, in particular, the tunable three-dimensional calix[4]arenes, have been extensively investigated as potential artificial hosts for chiral recognition[24] and as efficient ligands and organocatalysts in catalytic systems like Suzuki–Miyaura cross-coupling,

[a] *School of Medicine, Huanghuai University, Zhumadian 463000, Henan, P. R. China*
[b] *Department of Chemistry, University of Cambridge, Lensfield Road, Cambridge, CB2 1EW, UK. E-mail: spring@ch.cam.ac.uk*
[c] *Department of Chemistry, Zhejiang University, Hangzhou 310027, Zhejiang, P. R. China. E-mail: bfshi@zju.edu.cn*
[d] *School of Pharmacy, Hangzhou Medical College, Hangzhou 310014, Zhejiang, P. R. China. E-mail: zhangfengzhi@hmc.edu.cn*

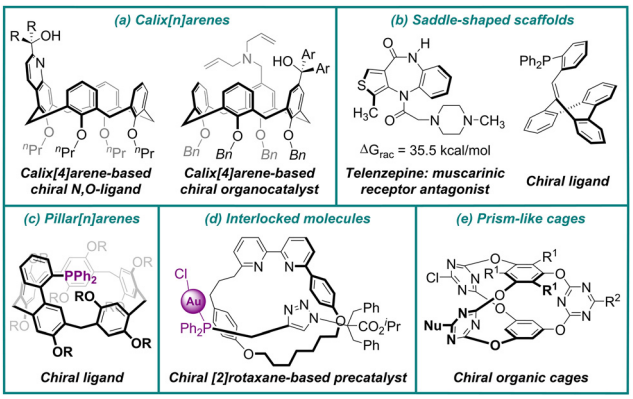

Fig. 1 Selected examples of inherently chiral scaffolds.

Tsuji–Trost allylic substitution, Henry reaction and Michael addition, *etc.* (Fig. 1a).[25,26] Furthermore, the seven-membered saddle-shaped heterocycle telenzepine was found to exhibit significant antimuscarinic activity, where the (+)-enantiomer was 500 times more potent than its (−)-enantiomer, which demonstrated the importance of their enantioselective synthesis (Fig. 1b).[27,28]

Owing to their intriguing structural properties and diverse applications, significant efforts have been dedicated to the enantioselective construction of these chiral architectures. Nevertheless, access to these enantiopure entities still predominantly relies on inefficient and tedious optical resolutions of racemic samples by means of chiral chromatographic techniques or with stoichiometric amounts of chiral auxiliaries. It is worth mentioning that, over the past few years, among the plethora of accomplishments reported, the catalytic asymmetric strategy has been emerging as one of the most efficient and sustainable approaches. This protocol provides a powerful platform to generate the inherently chiral scaffolds with structural diversity and enantiomeric purity, thus enabling

Kai Zhu

Kai Zhu received his PhD (2020) from Zhejiang University of Technology under Professor Fengzhi Zhang. After postdoctoral work with Professor Fengzhi Zhang (2020–2022) at the same university, he took up a faculty position at Huanghuai University. His research interests include the discovery of novel catalytic enantioselective reactions and their synthetic applications.

David R. Spring

David Spring is currently Professor of Chemistry and Chemical Biology at the University of Cambridge within the Chemistry Department. He received his DPhil (1998) from Oxford University under Sir Jack Baldwin. He then worked as a Wellcome Trust Postdoctoral Fellow at Harvard University with Stuart Schreiber (1999–2001), after which he joined the faculty at the University of Cambridge. His research programme is focused on the use of chemistry to explore biology.

Bing-Feng Shi

Bing-Feng Shi received his BS degree from Nankai University in 2001 and a PhD degree from the Shanghai Institute of Organic Chemistry, Chinese Academy of Sciences under the guidance of Professor Biao Yu in 2006. Following time as a postdoctoral fellow at the University of California, San Diego (2006–2007), he moved to The Scripps Research Institute working with Professor Jin-Quan Yu as a research associate. In 2010, he joined the Department of Chemistry at Zhejiang University as a professor. His research focus is on transition metal-catalyzed C–H functionalization and its application in the synthesis of biologically important small molecules.

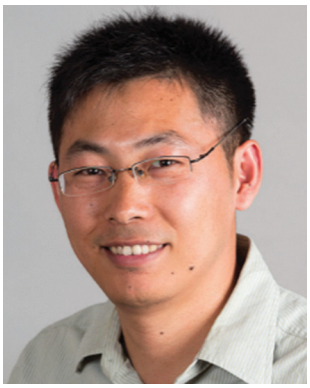

Fengzhi Zhang

Fengzhi Zhang received his MSc (2003) from Lanzhou University with Prof. Yulin Li and PhD (2008) from the University of Nottingham (UK) with Prof. Nigel Simpkins. He then worked with Profs. John Moses (2008–2009, Nottingham), Mike Greaney (2009–2011, Edinburgh), Matthew Gaunt (2011–2013, Cambridge) and David Spring (2013–2014, Cambridge) before he took up a faculty position at Zhejiang University of Technology (2014, China). Currently, he is a full professor at Hangzhou Medical College, and his research interests include the asymmetric synthesis, electrochemical synthesis, green chemistry and medicinal chemistry.

the expansion of their chemical space and potential applications.[11,15,17,20,29]

In 2023, Yang and co-workers provided a timely summary of advancements in the catalytic asymmetric synthesis of inherently chiral scaffolds.[29] Since then, numerous elegant works related to the catalytic asymmetric construction of such scaffolds have emerged. Additionally, several recent reviews have organized prior research and specialized perspectives according to specific compound classes.[11,15,17,20]

However, a comprehensive review that systematically summarizes and discusses all advancements in this rapidly evolving field remains lacking. Therefore, a comprehensive overview of this burgeoning research area is highly desirable. In this review article, we aim to systematically generalize the booming and remarkable advancements in the catalytic enantioselective synthesis of inherently chiral scaffolds, including calix[*n*]arenes, pillar[*n*]arenes, saddle-shaped scaffolds, mechanically interlocked molecules, and prism-like cages, in which the molecular chirality results when the stereogenic unit is the entire molecular scaffold itself, rather than localized stereogenic elements. We anticipate that this tutorial review will offer valuable insights for future research on the rational design of conceptually novel and streamlined asymmetric synthetic systems, thereby expanding the chemical space of inherently chiral scaffolds and improving the added value of these molecules.

2. Enantioselective construction of calixarenes

Inherently chiral calixarenes, a highly attractive type of privileged macrocyclic structures, exhibit broad applications in chiral recognition and sensing, circularly polarized luminescence, asymmetric catalysis, and separation science.[8–11,24–26] In general, inherent chirality can be introduced into the calixarene platform in a sophisticated manner by incorporation of achiral substituents into the bridging units, or upper- and/or lower-rim. In most cases, approaches for stereocontrolled preparation of these scaffolds are primarily limited to chiral auxiliary-based resolutions and couplings, often suffering from poor atom economy and low efficiency. Catalytic enantioselective synthesis, which can be considered to be a powerful and versatile synthetic method for accessing enantioenriched calixarenes, remains a longstanding challenge and is still in its infancy.[11]

2.1. Biocatalytic approach

To meet the demands of both economic value and high efficiency, earliest attempts toward the catalytic pathways were focused on the enzymatic reactions. In 1998, McKervey and colleagues discovered that the acylation of achiral triethyl alcohol monophenols **1** with acylating agent vinyl acetate **2** can be promoted by the cross-linked enzyme crystals (CLECs) of *Aspergillus niger* lipase to derive optically pure monoacetylated calix[4]arenes **3** with high to excellent enantioselectivities, albeit in poor yields (Scheme 1).[30]

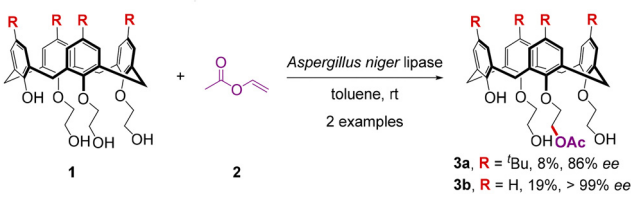

Scheme 1 Biocatalytic synthesis of enantiopure calix[4]arenes *via* enantioselective desymmetrization.

These results demonstrate the importance of enzymatic catalysis as a means to effect asymmetric synthesis of large, inherently chiral calixarenes. After McKervey and co-workers disclosed the biocatalytic access to enantiopure calix[4]arenes *via* an enantioselective desymmetrization reaction, it took more than a decade to see another catalytic method leading to the inherently chiral azacalix[4]arene.

2.2. Transition-metal-catalyzed methods

2.2.1. Enantioselective macrocyclization. The enantioselective Buchwald–Hartwig aryl amination reaction has received massive interest for its manifold applications in the construction of valuable chiral structures.[31,32] In 2009, Tsue and colleagues developed an asymmetric palladium-catalyzed intramolecular Buchwald–Hartwig cyclization reaction of *N*′,*N*″-tribenzylated acyclic tetramer **4** for the preparation of inherently chiral azacalix[4]arene **5** (Scheme 2).[33] Among various chiral ligands, it was found that (*R*)-SEGPHOS was the most effective one for the stereocontrol, although the enantioselectivity (35% ee) is unsatisfactory. After further purification by recrystallization, azacalix[4]arene **5** can be prepared with 99% ee.

In 2020, Wang, Tong and co-workers used a similar strategy for the catalytic enantioselective intramolecular C–N coupling of ABCD-type linear tetramer **6** to produce inherently chiral heteracalix[4]aromatics **7** (Scheme 3).[34]

The asymmetric macrocyclization promoted by a palladium/(R,S_p)-JOSIPHOS complex afforded ABCD-type inherently chiral tetraazacalix[4]aromatics **7** in moderate to good yields (up to 67%) and generally excellent enantiomeric excesses (up to >99% ee). Density functional theory (DFT) calculations revealed that the activation free energy of transition state **TS-1**

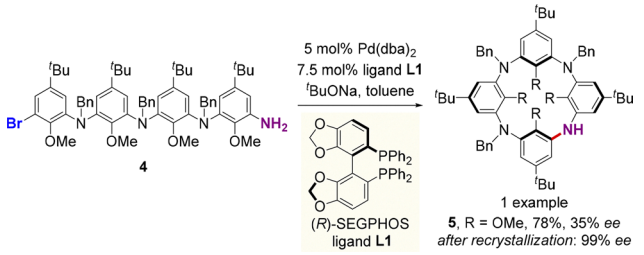

Scheme 2 Palladium-catalyzed enantioselective synthesis of azacalix[4]arene *via* intramolecular Buchwald–Hartwig cyclization.

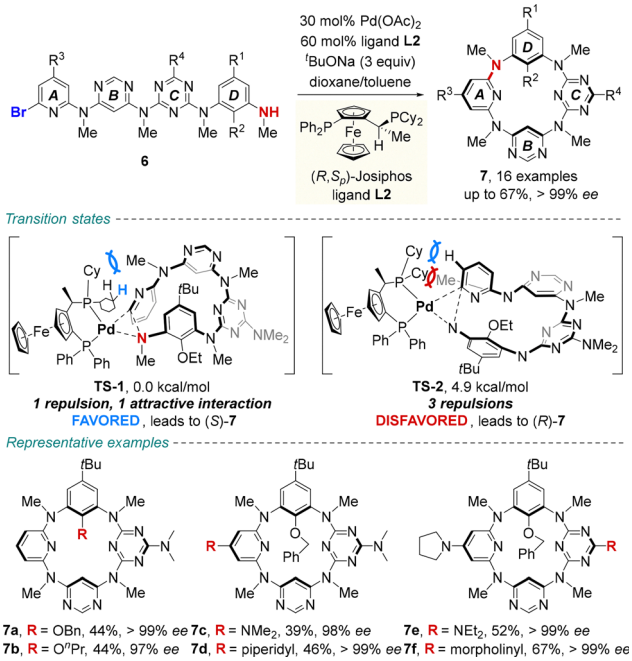

Scheme 3 Palladium-catalyzed enantioselective synthesis of ABCD-type inherently chiral tetraazacalix[4]aromatics.

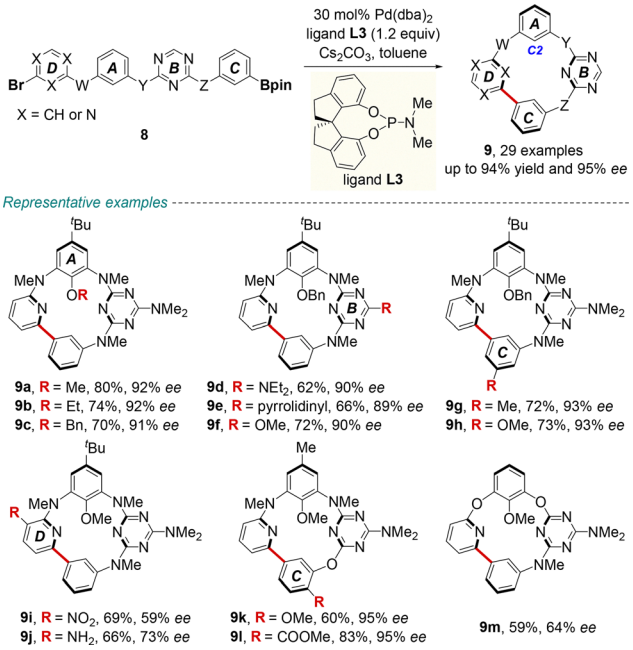

Scheme 4 Pd-catalyzed enantioselective synthesis of inherently chiral nor-heteracalixarenes *via* intramolecular Suzuki–Miyaura coupling.

is lower than that of **TS-2**. In the (*S*)-pathway, the favorable C–H···π interaction, along with weaker steric repulsion between cyclohexyl substituents on the ligand and the *N*-methyl group of substrate **6**, is thought to efficiently stabilize the unique transition state geometry, thereby governing the enantiocontrol. Remarkably, the acquired enantiomerically enriched macrocycles showed excellent, pH-triggered switchable electronic circular dichroism (ECD) and circularly polarized luminescence (CPL) properties. These inherently chiral macrocycles are poised to serve as guest-responsive chiroptical systems by leveraging the versatile molecular recognition capabilities of heteracalix[4]aromatics.

Palladium-catalyzed asymmetric Suzuki–Miyaura couplings have traditionally been employed to generate axial chirality through the stereoselective construction of aryl–aryl bonds.[35] Recently, Tong and colleagues applied this approach for the preparation of inherently chiral macrocycles (Scheme 4).[36]

With the linear achiral precursor as the substrate, represented as **8** in Scheme 4, in the presence of the chiral phosphoramidite ligand (*R*)-SIPHOS (**L3**), the intramolecular Pd-catalyzed Suzuki–Miyaura cross-coupling macrocyclization reaction afforded the corresponding 15-membered inherently chiral nor-heteracalixarenes **9** in good to high yields and enantioselectivities. Racemization studies revealed that the restricted rotation of the aromatic ring A and the steric effect of the C2 substituents determine the configurational stability of the inherent chirality. Moreover, the intriguing chiroptical properties of these rigid molecules, including high fluorescence quantum yields and CPL brightness values (B_{CPL}, up to 0.65), made them a promising platform for fabricating CPL emitters.

2.2.2. Enantioselective desymmetrization. In 2022, a prominent report by Cai and colleagues documented the highly enantioselective intramolecular C–H arylation of various prochiral calix[4]arenes **10** (Scheme 5).[37] Promoted by a catalyst system comprising palladium(0) complex and chiral bifunctional

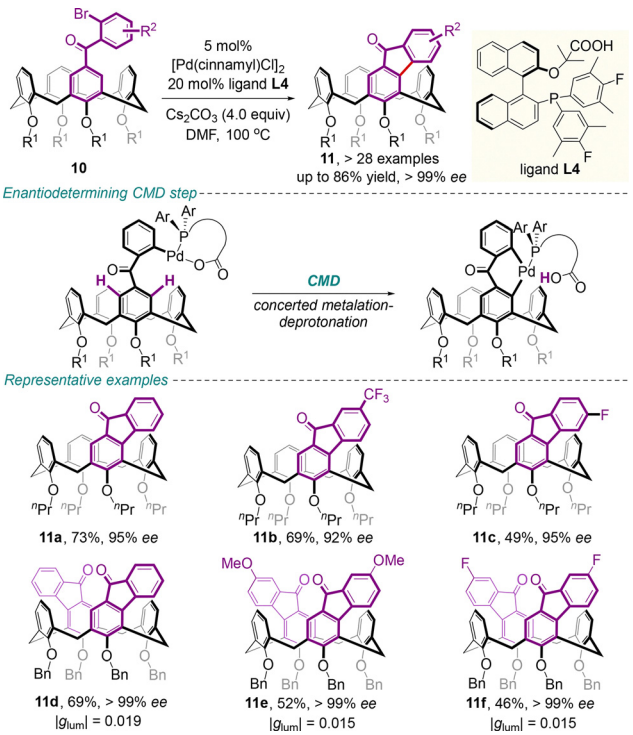

Scheme 5 Palladium-catalyzed enantioselective synthesis of inherently chiral calix[4]arenes *via* intramolecular C–H arylations.

phosphine-carboxylate ligand **L4**, a broad set of inherently chiral calix[4]arenes **11** with fluorenone motifs were obtained in good to high yields (up to 86% yield) with high to excellent enantioselectivities (up to >99% ee). Control experiments indicated that the synergistic effect of the carboxylate and phosphorus moieties in the bifunctional ligand **L4** is crucial for the enantiodetermining concerted metalation–deprotonation (CMD) step. Furthermore, bis-fluorenone products **11d–11f** were obtained *via* twofold cyclization in good yields and higher enantiomeric excess (>99% ee), likely due to kinetic resolution occurring at the second intramolecular C–H arylation step. Notably, these inherently chiral calix[4]arenes, functionalized with two fluorenone motifs, exhibit extraordinarily high luminescence dissymmetry factors ($|g_{lum}|$ = 0.015–0.019), underscoring the significant potential of inherent chirality for developing organic optoelectronic materials.

Concurrently, from the same starting materials **10**, Tong and colleagues reported an alternative palladium-catalyzed sequential intramolecular transannular dehydrogenative coupling reaction (Scheme 6).[38] With this protocol, a wide range of 9*H*-fluorene-embedded inherently chiral calixarenes **12** were obtained in good yields with high enantioselectivities using $PdBr_2$ as the catalyst and chiral phosphoramidite **L5** as the ligand. The absolute configuration of **12a** was confirmed by X-ray crystallography analysis. Mechanistically, the reaction might initiate from the oxidative addition of Pd/**L5** with **10**, followed by asymmetric C–H activation/1,5-palladium migration to form **int-1**, which would undergo a second C–H activation/reductive elimination to deliver the final *meta–meta* bridged calix[4]arenes **12**. These highly rigid structures exhibit unique chiroptical properties.

Very recently, Zhou, Cheng and co-workers inventively designed an efficient palladium/chiral norbornene cooperative catalyzed enantioselective Catellani-type cascade reaction for the synthesis of enantiomerically enriched calix[4]arenes **15**

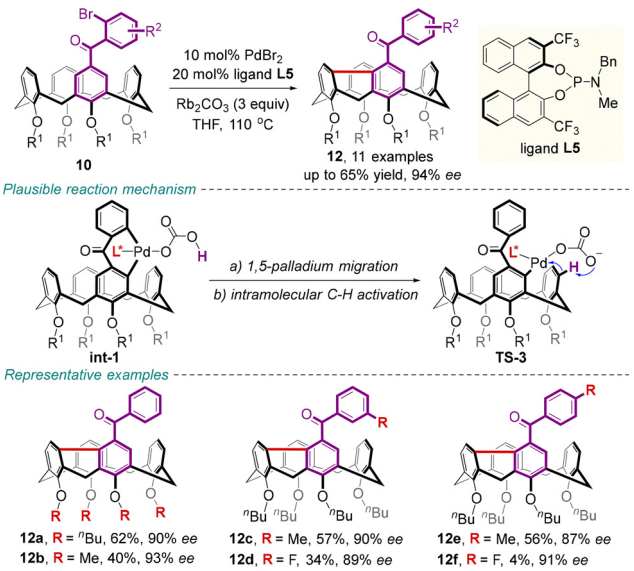

Scheme 6 Palladium-catalyzed enantioselective synthesis of inherently chiral calixarenes *via* transannular dehydrogenative coupling.

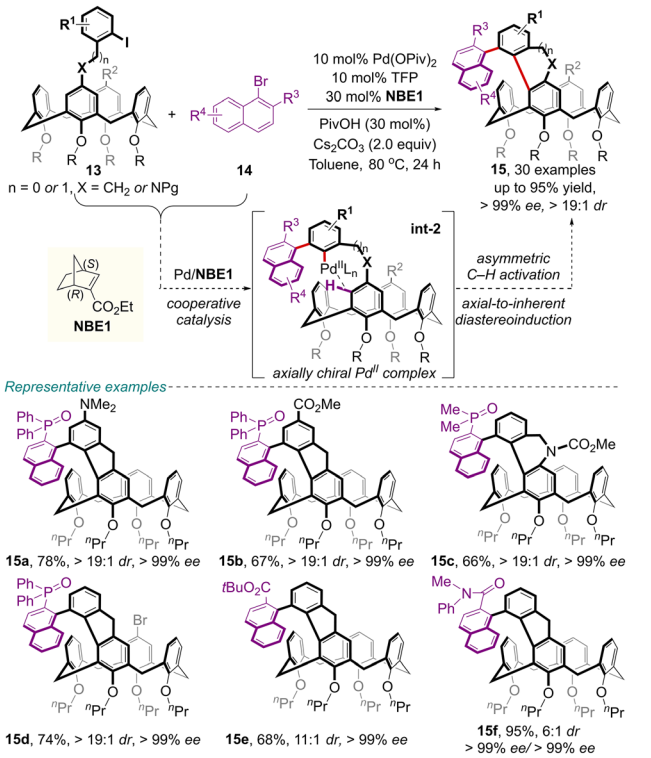

Scheme 7 Palladium/chiral norbornene cooperative catalyzed enantioselective method for the synthesis of calix[4]arenes featuring both axial and inherent chirality.

featuring both axial and inherent chirality with excellent diastereo- and enantioselectivities (Scheme 7).[39]

The suggested reaction pathway involves the formation of axially chiral Pd^{II} complex **int-2**, which undergoes an asymmetric intramolecular C–H activation process and realizes the axial-to-inherent chirality conversion. This class of phosphine oxide-substituted calix[4]arenes **15** with axial and inherent chirality could be facilely transformed into a novel chiral phosphine ligand, which exhibits high catalytic activity in the silver-catalyzed enantioselective [3+2] cyclization reaction.

Regarding the key importance of cavitands as privileged scaffolds in supramolecular chemistry, their enantioselective preparation has attracted considerable attention.[40,41] More recently, Zhu, Gandon and co-workers achieved the synthesis of inherently chiral resorcinarene cavitands **17** in modest to good yields and high enantiomeric excess by engineering an ionic chiral palladium-catalyzed cross-coupling of the corresponding prochiral cavitands **16** (Scheme 8).[42] Using $Pd_2(dba)_3$ and amino acid-derived ligand **L6** as the catalyst system, the authors developed conditions for stereoselective Suzuki–Miyaura coupling, Buchwald–Hartwig amination, and Sonogashira coupling reactions with a variety of coupling partners. Mechanistic studies revealed that synergistic electrostatic steering, along with electrostatic catalysis by the interactions between the ionic catalyst and the substrate, could be responsible for the selectivity control observed. Additionally, based on these chiral catalytic systems, a hierarchical heterofunctionalization protocol

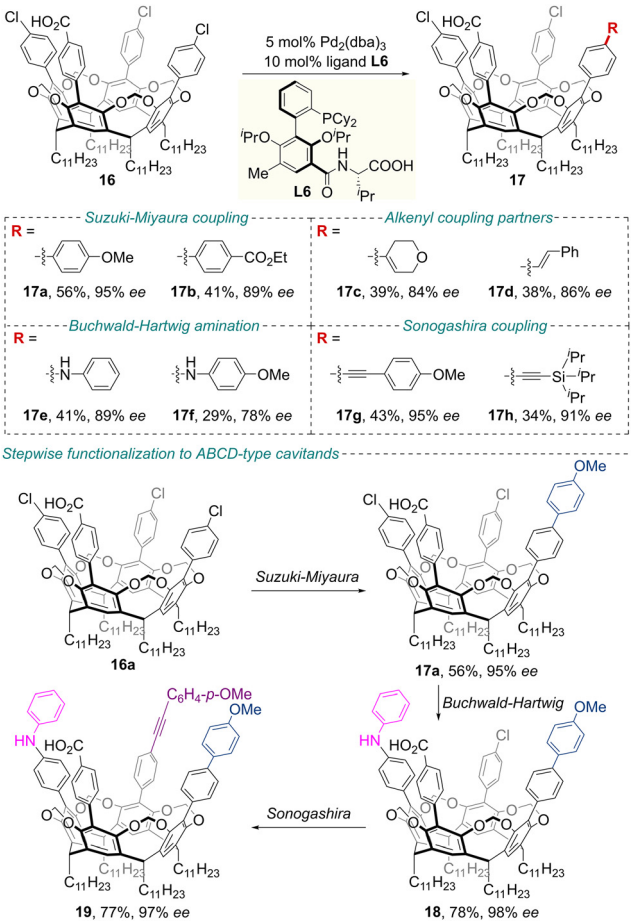

Scheme 8 Ionic chiral palladium-catalyzed desymmetrizing cross-coupling to inherently chiral resorcinarene cavitands.

was designed for the enantioselective construction of functionalized inherently chiral ABCD-type cavitands, which bear programmable substitution patterns, through sequential cross-coupling reactions. Using the products thus synthesized, a chiral hemicarcerand was designed that exhibits enantioselective binding toward a BINOL-derived guest through specific host–guest interactions. This system demonstrates efficient discrimination of nanometer-sized enantiomers, underscoring its potential as an artificial chiral receptor.

In 2023, Cera, Secchi and co-workers reported the synthesis of inherently chiral calix[4]arenes **21** *via* a step- and atom-economical, gold(I)-catalyzed intramolecular hydroarylation of alkynes **20** (Scheme 9).[43] Nevertheless, the corresponding catalytic enantioselective version of this method was not fruitful, and only a single example was presented with 98% yield and 28% ee.

Due to its less toxic and cost-efficient features, the cobalt-catalyzed asymmetric C–H activation strategy has garnered considerable attention for the synthesis of a panel of highly enantioenriched inherently chiral calix[4]arenes.[44]

Very recently, Niu, Yang and colleagues unraveled that the utilization of a chiral salicyloxazoline (Salox) ligand **L7** for the cobalt-catalyzed enantioselective intermolecular C–H

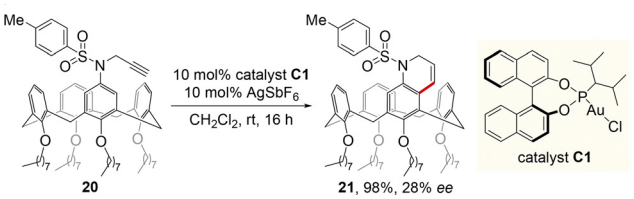

Scheme 9 Gold-catalyzed asymmetric synthesis of inherently chiral calix[4]arenes *via* intramolecular hydroarylation of alkynes.

activation/annulation of benzamide tethered calix[4]arenes **22** with exogenous alkynes **23** provided the inherently chiral products **24**, with multiple C–N axial chirality, in good to high yields (up to 94%) with excellent diastereoselectivity (all $>20:1$ dr) and high enantioselectivity (up to 96% ee) (Scheme 10).[45] The utility of this protocol was highlighted by the gram-scale reaction, synthetic transformations and catalytic application. Additionally, compound **24a** effectively functions as a host molecule for the enantioselective recognition of C_2 symmetric chiral binaphthols, demonstrating its potential for applications in chiral discrimination. The proposed catalytic cycle initiates with the coordination of chiral ligand **L7** to Co(II) and undergoes oxidation with O_2 to generate the active Co(III) species. Subsequent coordination with substrate **22** is followed by chelation of the *N*-oxide group to the cobalt center. This key interaction helps organize a rigid chiral environment through synergy with ligand **L7**, thereby controlling the enantioselectivity

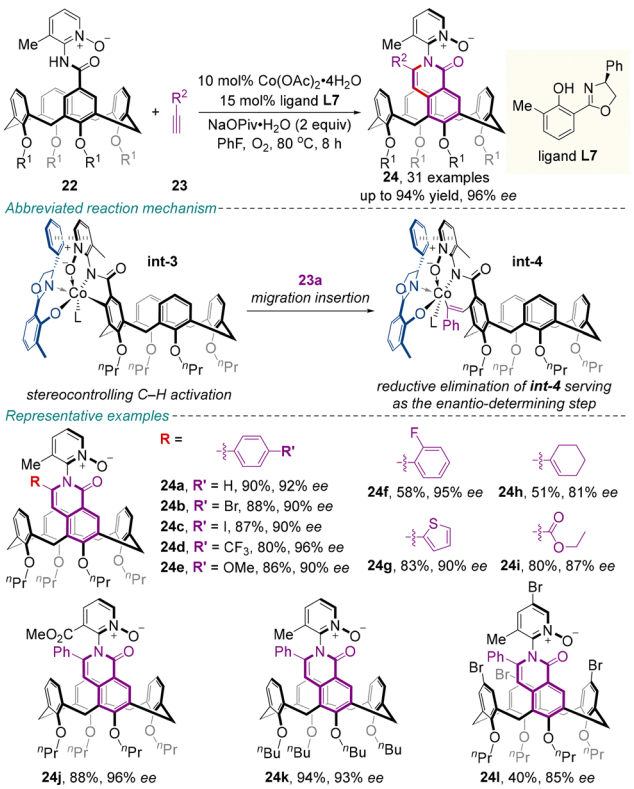

Scheme 10 Cobalt-catalyzed asymmetric C–H activation/annulation strategy for the synthesis of calix[4]arenes featuring both inherent and axial chirality elements.

during C–H activation and alkyne **23** migratory insertion. Reductive elimination then affords the product as well as the Co(I) species, which is reoxidized to the active Co(III) catalyst by O_2 to complete the catalytic cycle.

Almost simultaneously, a similar transformation was independently accomplished by Shi and co-workers using different chiral Salox ligands (**L8**, **L9**) and directing groups (8-aminoquinoline derivatives) (Scheme 11).[46] In terms of the substrate scope, acetylene gas, ethylene gas, substituted aryl/alkyl alkynes, and allene were all well tolerated, resulting in the formation of a remarkably broad range of inherently or both inherently and axially chiral calix[4]arenes **27** in high to excellent yields (up to 99%) with excellent enantioselectivities (up to >99% ee). Confirmed by the single-crystal X-ray diffraction of cobaltacyle and previous investigations,[44] the π–π interaction between quinolyl in the substrate and phenyl in the Salox ligand was characterized as a dominant factor for outstanding stereocontrol. Moreover, the measured photophysical properties of these products indicate their potential applications in organic optoelectronic materials science.

In recent years, the renaissance of organic electrosynthesis has given new impetus to catalytic enantioselective synthesis.[47–49] In the same report, Shi further implemented an electrochemical asymmetric synthetic version of this catalytic system and delivered the desired products **27** with high yields (74–91%) and enantioselectivities (87–93% ee), which avoided the drawbacks posed by the employment of stoichiometric sacrificial chemical oxidant $Mn(OAc)_3{\cdot}2H_2O$ (Scheme 12).

Meanwhile, Niu, Dou and colleagues demonstrated an elegant example of electrochemically driven cobalt-catalyzed

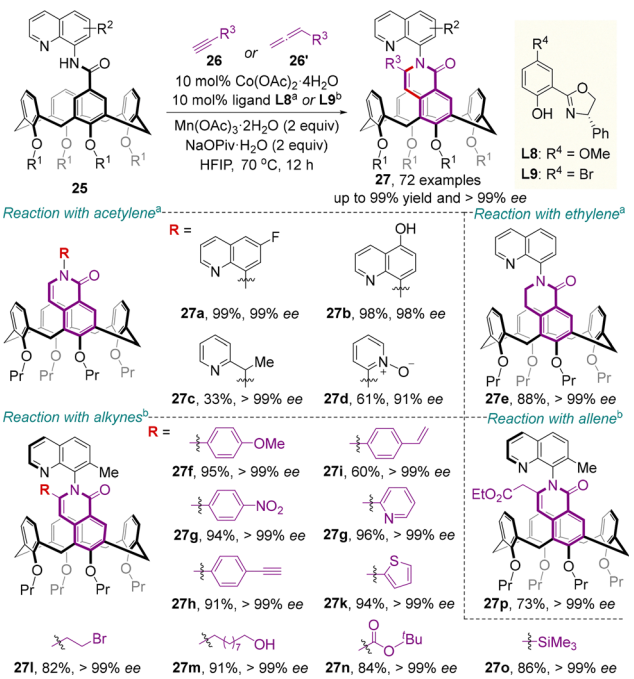

Scheme 11 Shi's cobalt-catalyzed enantioselective intermolecular C–H annulation strategy for the synthesis of calix[4]arenes with inherent or both inherent and axial chirality.

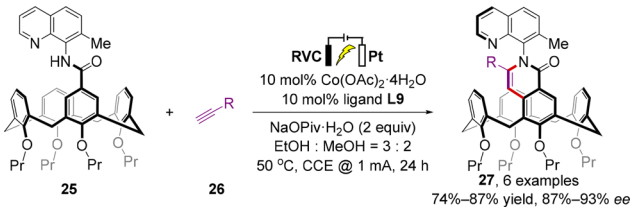

Scheme 12 Electrochemically driven cobalt-catalyzed enantioselective intermolecular C–H annulation strategy.

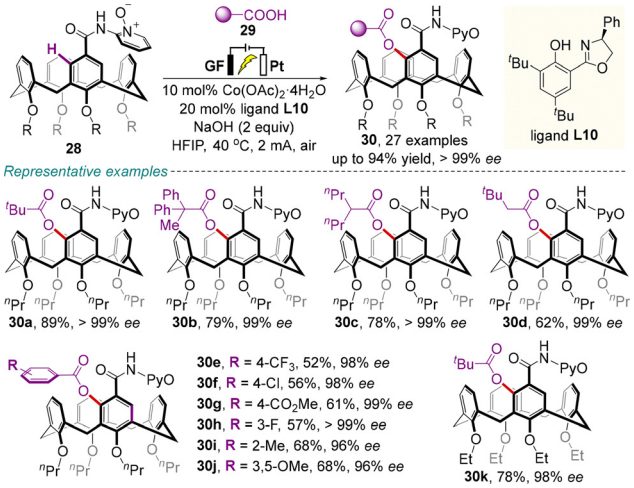

Scheme 13 Electrochemically driven cobalt-catalyzed asymmetric C–H acyloxylation for the synthesis of inherently chiral calix[4]arenes.

asymmetric aryl C–H acyloxylation of prochiral calix[4]arenes **28**, enabling the generation of various enantioenriched inherently chiral acyloxylated products **30** with good to high yields (up to 94%) and excellent enantioselectivities (up to >99% ee) (Scheme 13).[50] The success of this protocol was attributed to the combination of the directing group pyridine *N*-oxide with chiral Salox ligand **L10**, as well as the perfect match of electrochemistry with chiral cobalt catalysts.

2.2.3. Kinetic resolution. Enantioenriched zigzag-type C_4-symmetric molecular belts **32** were elegantly fabricated by Wang, Tong and colleagues under copper/H_8-binaphthol-catalyzed kinetic resolution (KR) and subsequent cyclization of racemic resorcin[4]arenes **31** (Scheme 14).[51] The substituents on the chiral ligand have a significant impact on the stereocontrol of belt product **32** and remaining starting material **31**. By utilizing H_8-BINOL ligand **L11**, the starting material **31** was recovered in 23% yield with 98% ee, while application of 3,3′-dibromosubstituted H_8-BINOL ligand **L12** furnished *M*-**32** with up to 92% ee. The rigidification from the fluxional macrocycle **31** to belt **32** markedly enhanced both chiroptical and photophysical properties. This transformation establishes a robust strategy for assembling chiral molecular belts and advancing functional chiroptical materials.

2.3. Organocatalytic strategy

2.3.1. Enantioselective macrocyclization. Chiral phosphoric acids (CPAs) have been used as organocatalysts for a wide

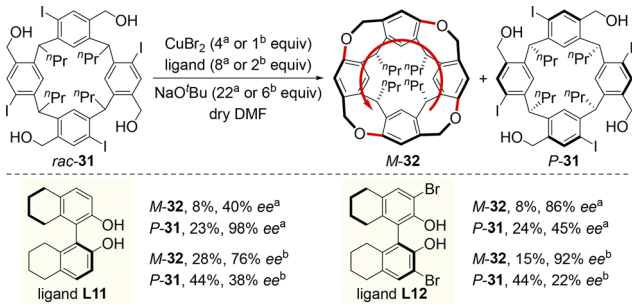

Scheme 14 Copper-catalyzed asymmetric synthesis of inherently chiral zigzag-type molecular belt *via* KR and subsequent cyclization.

range of asymmetric *C*-heteroatom bond-forming reactions.[52–54] Recently, Wang, Tong, Cheng and co-workers constructed highly enantiopure inherently chiral heteracalix[4]aromatics, N_3,*O*-calix[2]arene[2]triazines **34** with up to 97% ee through intramolecular nucleophilic aromatic substitution (S_NAr) of linear precursors **33** catalyzed by **CPA1**, albeit in moderate yields (Scheme 15).[55] Multiple non-covalent bond interactions between substrate **33** and chiral catalyst **CPA1** markedly reinforced the enantioselective macrocyclization process. The secondary amino-*s*-triazine moiety of **33** contributed to reaction efficiency and enantioselectivity. A substrate without the N–H binding site in the bridging position merely gave the corresponding product **34g** only in 7% yield with 42% ee.

This strategy has been further extended to assemble inherently chiral tetraazacalix[4]aromatics using **CPA2** as the catalyst by Wang, Cheng and colleagues recently (Scheme 16).[56] It should be pointed out that the inherent chirality of the resulting tetraazacalix[1]arene[1]pyridine[2]triazines **36** originated

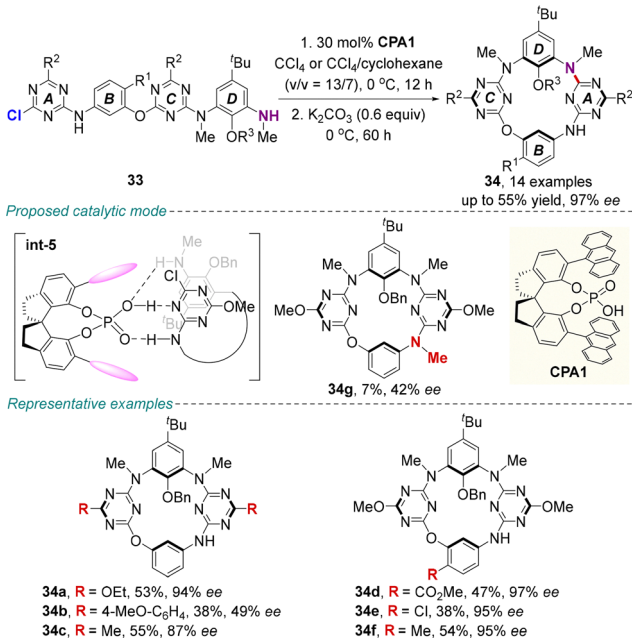

Scheme 15 CPA-catalyzed enantioselective synthesis of inherently chiral N_3,*O*-calix[2]arene[2]triazines *via* an intramolecular S_NAr reaction.

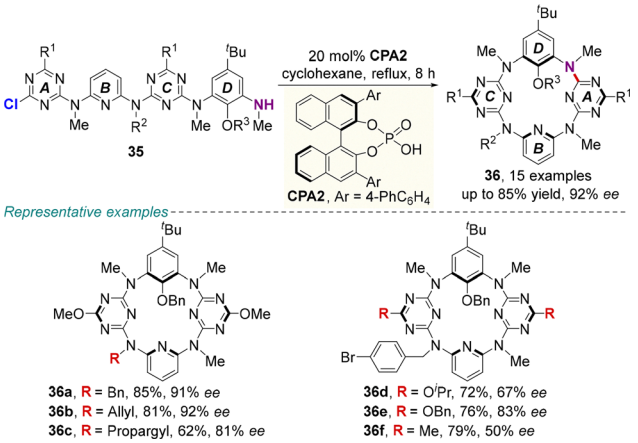

Scheme 16 CPA-catalyzed asymmetric synthesis of inherently chiral tetraazacalix[4]aromatics *via* an intramolecular S_NAr reaction.

from the variation of a single substituent at the bridging nitrogen units.

Furthermore, Tong and colleagues demonstrated that the S_NAr reaction could be applied in an intermolecular macrocyclic condensation process (Scheme 17).[57] Applying cinchonine-derived chiral phase-transfer catalyst **PTC1**, the asymmetric one-pot cross-cyclotetramerization of 2,6-dichloro-3-nitropyridine **37** with resorcinol derivatives **38** delivered inherently chiral tetraoxacalix[2]arene[2]pyridines **39** with moderate to good enantioselectivities (up to 77% ee). However, poor yields were obtained, potentially due to the complexity of the multiple competing reaction pathways.

2.3.2. Enantioselective desymmetrization. In recent years, the CPA-catalyzed asymmetric multicomponent Povarov reaction has become a powerful strategy to forge and control central chirality, axial chirality and helical chirality.[58–60]

Recently, by employing this strategy, Liu's group and Yang's group independently realized the enantioselective synthesis of inherently chiral calix[4]arenes, through an effective central-to-inherent chirality conversion paradigm (Scheme 18).[61,62] Under different CPA (**CPA3** or **CPA4**) catalysis, amino group-substituted calix[4]arenes **40**, (di)enamides **41** and aldehydes **42** underwent an asymmetric Povarov-type annulation to generate the key optically enriched cycloadduct with two well-defined carbon stereocenters, which was oxidized with DDQ to obtain a diverse array of novel inherently chiral 4-amido-quinoline-containing calix[4]arenes **43** or **44** with excellent enantioselectivities (up to 99% ee). Mechanistic studies assumed that the high selectivity

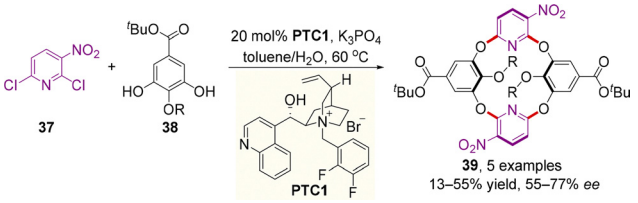

Scheme 17 PTC-catalyzed enantioselective synthesis of inherently chiral tetraoxacalix[2]arene[2]pyridines *via* cross-cyclotetramerization.

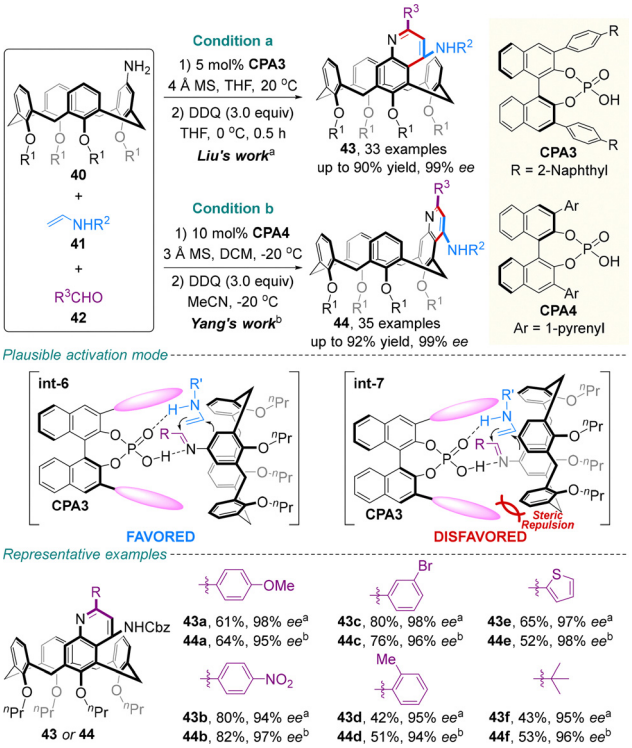

Scheme 18 CPA-catalyzed asymmetric synthesis of chiral 4-amido-quinoline-containing calix[4]arenes *via* the Povarov reaction.

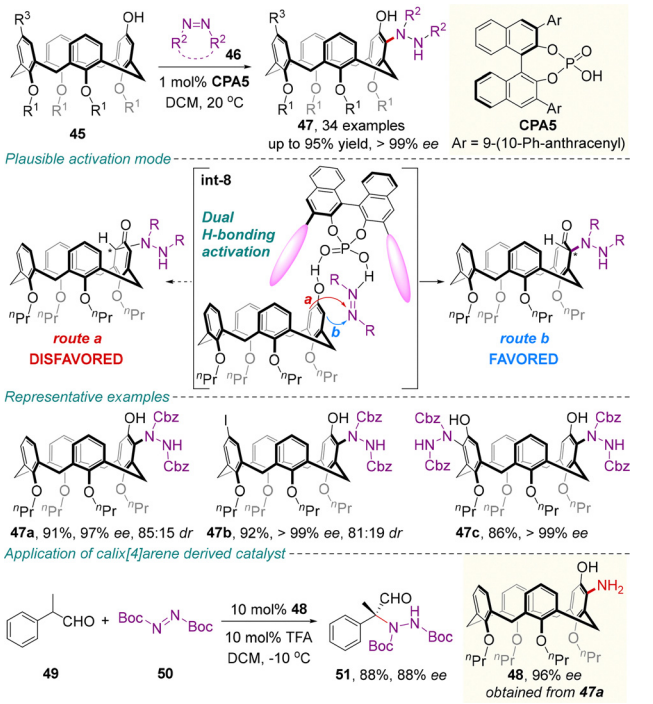

Scheme 19 CPA-catalyzed asymmetric synthesis of inherently chiral calix[4]arenes *via* electrophilic aromatic aminations.

arises from the steric repulsions between the vertical plane of calix[4]arenes **40** and the bulky aryl substituents on the CPA catalyst.

Very recently, Yang and co-workers successfully accomplished the enantioselective synthesis of inherently chiral calix[4]arenes **47** through CPA-catalyzed asymmetric electrophilic aromatic aminations of phenol-containing prochiral calix[4]arenes **45** with high to excellent yields and enantioselectivities (Scheme 19).[63]

This transformation evolves through CPA-controlled stereoselective addition to produce a stereoenriched dearomatized intermediate with both central and inherent chirality. Rapid keto–enol tautomerism follows with central-to-inherent chirality conversion to render the *ortho*-C–H aminated phenol products **47** stereochemically defined. In analogy with the previous research on the origin of enantioselectivity, the parallel alignment of the substrates relative to one of the catalyst's anthracenyl groups, along with a series of C–H···π interactions between the reactant and the anthracenyl group, is probably responsible for the enantiocontrol. Moreover, the chiral *meta*-amino-substituted calix[4]arene **47a** was readily converted into the primary amine catalyst **48**. This novel catalyst efficiently promoted the asymmetric α-amination of aldehyde **49** with azodicarboxylate **50**, highlighting its significant potential for the development of useful chiral organocatalysts.

In 2024, Chen and colleagues developed an efficient chiral Lewis base-catalyzed desymmetrization approach for the enantioselective electrophilic sulfenylation of various prochiral

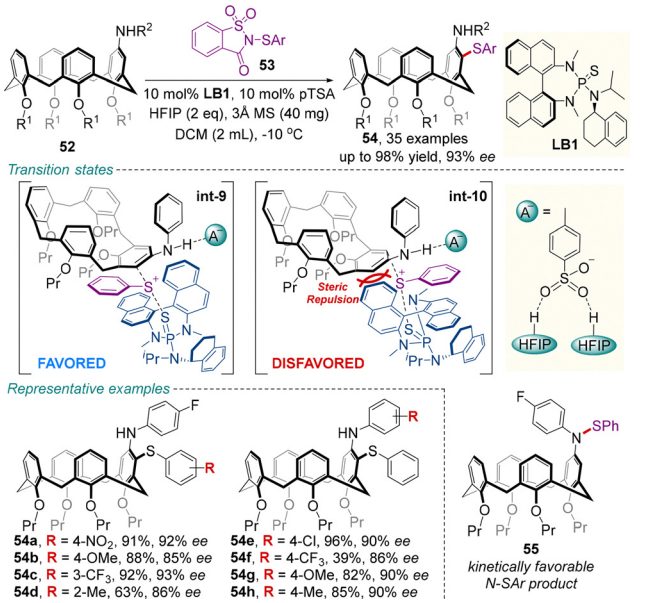

Scheme 20 Chiral sulfide catalyzed desymmetrizing electrophilic sulfenylation of racemic calix[4]arenes.

calix[4]arenes **52** (Scheme 20).[64] Upon treatment with sulfenylating reagent **53**, 10 mol% of sulfide catalyst **LB1**, and hexafluoroisopropanol (HFIP), the reaction proceeded smoothly to give the enantioenriched inherently chiral sulfur-containing calix[4]arenes **54** in moderate to excellent yields (most ≥80%) with high enantioselectivities (most ≥90% ee). Mechanistically, the thermodynamically favored *C*-SAr product **54** is gradually

formed from the rapidly formed kinetically favored *N*-SAr product **55**. In addition, the combination of the chiral Lewis base catalyst **LB1** and HFIP has a dramatic effect on both enantioselectivity and reactivity, since the hydrogen bonds between the *p*-toluenesulfonic acid (*p*TSA) anion/HFIP species (A^-) and the N–H moiety of substrate **52** may decrease the energy barrier of this transformation and contribute to stabilize the favorable transition state **int-9**.

Chiral NHC-catalyzed desymmetrization of prochiral diformyl derivatives stands out as a promising platform for asymmetric transformations. Recently, this chemistry was further popularized to access inherently chiral ABCC-type calix[4]arenes by Veselý, Dočekal and colleagues (Scheme 21).[65] Under oxidative conditions (tetra-*tert*-butyldiphenyl-quinone, DQ), the reaction of prochiral diformylcalix[4]arenes **56** with bifunctional chiral **NHC1** effectively generates an NHC-bound acylazolium intermediate **int-11**, which then reacts with aromatic alcohols **57** to complete the esterification process. Mechanistic investigations indicated that desymmetrization is the enantiodetermining step. Remarkably, this method has been applied for the late-stage modification of several natural products and bioactive compounds, including Umbelliferone, Mecarbinate, Carvacrol and Capsaicin, which furnished the desired drug-like molecules (**58k–58n**) with high yields (61–88%) and ee values (71–95% ee), showing good substrate tolerance.

More recently, Tong and co-workers reported that achiral resorcin[4]arenes **59** underwent a 4-fold Mannich/cyclization reaction to generate C_4-symmetric chiral resorcin[4]arenes **61** in the presence of chiral *N*,*N*′-dioxide **L_3-PiMe$_3$** derived from (*S*)-piperidine-2-carboxamide (Scheme 22).[66]

The desymmetrization of symmetric resorcin[4]arene **59** through the first Mannich/cyclization reaction enantioselectively formed the 1,3-oxazinane-fused resorcin[4]arene intermediate **int-12** of C_1 symmetry. This intermediate adopts a conformation

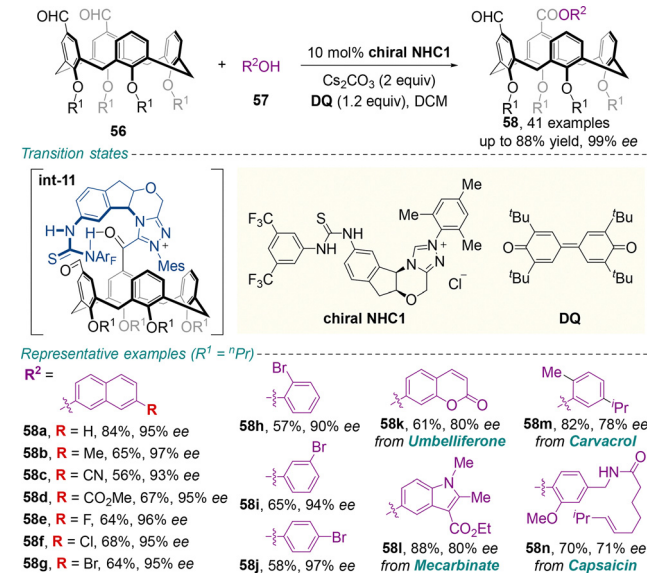

Scheme 21 Chiral NHC-catalyzed enantioselective desymmetric esterification of prochiral diformylcalix[4]arenes.

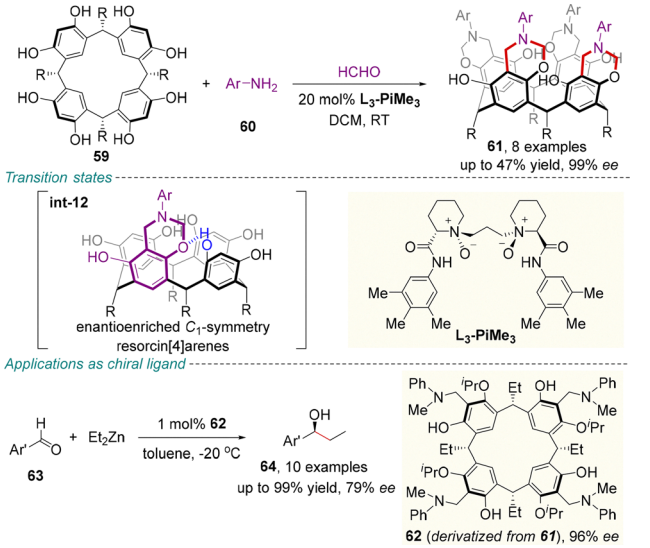

Scheme 22 *N*,*N*′-Dioxide catalyzed enantioselective desymmetrization of resorcin[4]arenes *via* the Mannich/cyclization reaction.

stabilized by intramolecular hydrogen bonding interaction, enabling exclusive regioselectivity during the subsequent transformation to afford C_4-symmetric products **61**. Furthermore, such chiral resorcin[4]arenes could be transformed into novel chiral catalysts for the asymmetric addition of diethylzinc to benzaldehyde. This system successfully demonstrated the effective transfer of inherent chirality from the macrocyclic scaffold to the product's central chirality, underscoring its potential in enantioselective catalysis.

2.3.3. (Dynamic) kinetic resolution. In 2023, seminal work on organocatalytic asymmetric synthesis of inherently chiral macrocycles through dynamic kinetic resolution (DKR) was exemplified by Sessler, Inokuma and colleagues (Scheme 23).[67] To prevent ring inversion of calix[1]furan[1]pyrrole[1]thiophene **65**, *N*-methylation of the pyrrole moiety was implemented under the control of chiral ammonium salt **PTC2**, thus affording calix[1]furan[1](*N*-methylpyrrol)[1]-thiophene **66** in 48% yield, albeit with low enantioselectivity.

In 2024, the dynamic kinetic resolution protocol was utilized by Tong and colleagues to access inherently chiral calix[4](het)arenes (Scheme 24).[68] The reaction of diazadioxacalix[2]arene[2]quinazolines **67** with bromomethylarenes **68** as alkylation partners and cinchonine-derived **PTC3** as the catalyst delivered highly enantioenriched **69** in excellent yields. Guided by DFT studies and observed stereochemical outcomes, the excellent enantiocontrol could be attributed to the host–guest-like interaction between the substrate and the catalyst.

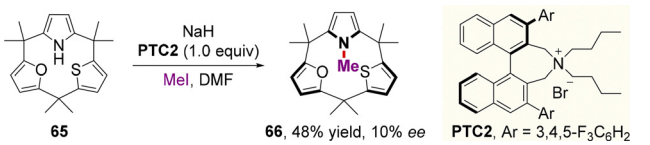

Scheme 23 Dynamic kinetic resolution (DKR) by enantioselective *N*-methylation of the pyrrole moiety.

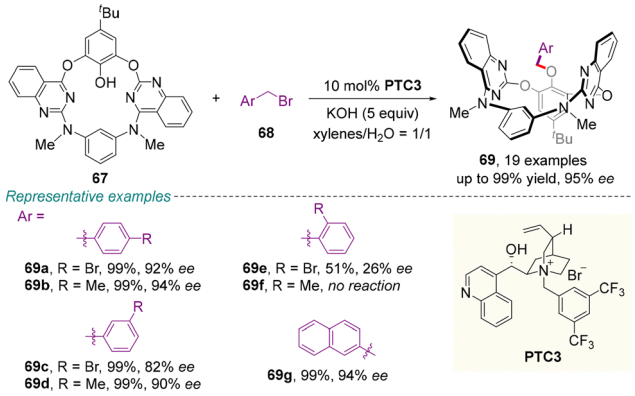

Scheme 24 Chiral PTC-catalyzed asymmetric synthesis of inherently chiral heteracalixarenes *via* dynamic kinetic resolution.

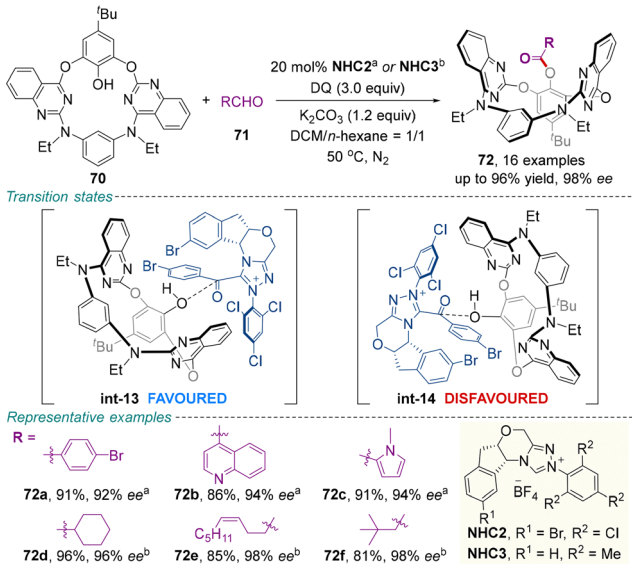

Scheme 25 Chiral NHC-catalyzed asymmetric synthesis of inherently chiral calix[4](het)arenes *via* dynamic kinetic resolution.

After the success of DKR in preparing inherently chiral macrocycles, Wang and co-workers implemented an NHC-catalyzed DKR protocol to forge inherently chiral heteracalixarenes **72** *via* esterification of diazadioxacalix[2]arene[2]quinazolines **70** (Scheme 25).[69] DFT analysis revealed that **int-13** exhibits a 9.2 kcal mol^{-1} lower energy barrier for hydroxyl addition to acyl azolium compared to **int-14**, kinetically favoring *S*-configured products. Furthermore, employing the same catalytic system, the kinetic resolution of racemic rac-**73** provided access to enantioenriched **74** with good to high enantioselectivities. Additionally, optically active ent-**73** was recovered in acceptable yields with high to excellent enantioselectivities (Scheme 26).

3. Enantioselective construction of pillar[*n*]arenes

Among various chiral macrocycles, pillar[*n*]arenes have garnered significant attention due to their unique topological

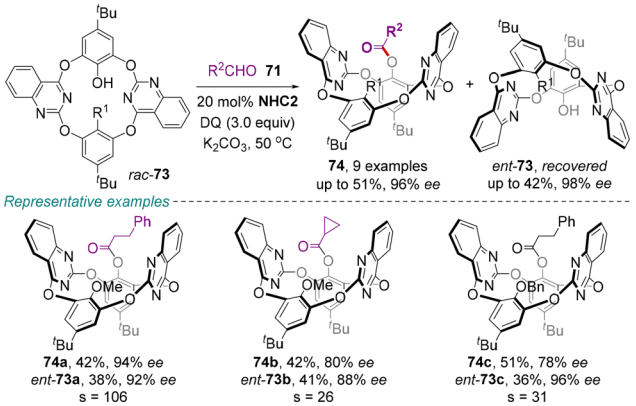

Scheme 26 Chiral NHC-catalyzed asymmetric synthesis of inherently chiral calix[4](het)arenes *via* kinetic resolution.

structures and broad utility in materials science,[70,71] host–guest chemistry,[72,73] and molecular machinery.[74,75] In particular, inherently chiral pillar[5]arenes, composed of five repeating paraphenylene methylene units, stand out for their synthetic accessibility and versatile functionality. However, free rotation of these repeating units leads to the coexistence of up to eight conformers in solution, presenting a major obstacle to obtaining configurationally stable enantiomers.[12–15] This dynamic behavior can be restrained through the introduction of sterically hindering substituents or the construction of mechanically interlocked and self-locking architectures, thereby enabling the isolation of stable enantiopure forms. Nevertheless, to date, the preparation of enantiopure pillar[5]arenes still predominantly relies on chiral HPLC resolution or diastereomeric crystallization, approaches that suffer from limited efficiency and scalability. Catalytic enantioselective synthesis offers an attractive alternative to overcome these drawbacks.

3.1. Enantioselective Sonogashira coupling

Recently, a breakthrough strategy for the enantioselective synthesis of inherently chiral pillar[5]arenes has been developed by Wang and co-workers *via* a Pd-catalyzed Sonogashira coupling reaction (Scheme 27).[76] This method enables efficient access to a diverse range of homo- and hetero-rimmed pillar[5]arenes **77** in good to high yields with high to excellent enantioselectivities (up to 97% ee). The absolute configuration of product **77a** was determined as a *pS* conformer by single-crystal X-ray diffraction. Notably, once the stereochemical configuration of one repeating unit in the pillar[5]arene framework is fixed as *pS* through the introduction of two sterically bulky alkynes, the remaining four units adopt the same chiral conformation through conformational induction, resulting in the all-*pS* conformer as the thermodynamically most stable enantiomer. Mechanistic studies revealed that the second Sonogashira coupling step is enantio-determining in this sequential double coupling process. Importantly, IRI (interaction region indicator) analysis indicated that reduced steric repulsion between the Pd center of catalyst Pd/**L13** and the phenyl group of the pillar[5]arene in transition state **int-15**

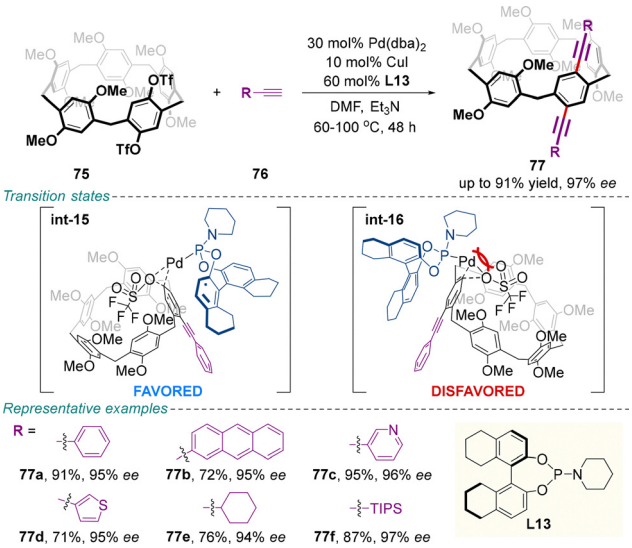

Scheme 27 Palladium-catalyzed asymmetric synthesis of inherently chiral pillar[5]arenes by DKR *via* Sonogashira coupling.

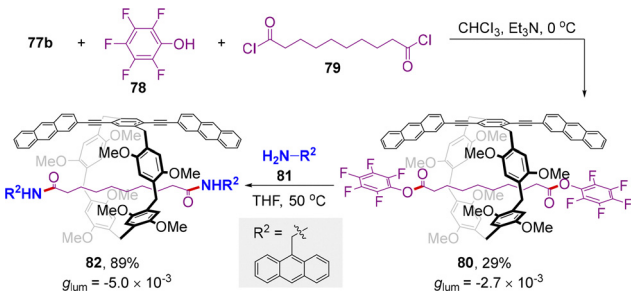

Scheme 28 Application of inherently chiral pillar[5]arene **77b** in the synthesis of chiral rotaxanes.

leads to a lower activation energy barrier, which is crucial for achieving high enantiocontrol. Furthermore, product **77b** was successfully employed as a chiral wheel component for the construction of chiral rotaxane **82**, which exhibits remarkable CPL with g_{lum} reaching up to −0.005 (Scheme 28).

3.2. Enantioselective Suzuki–Miyaura coupling

Very recently, Liu, Xi and colleagues disclosed a DKR based on the enantioselective Pd-catalyzed Suzuki–Miyaura coupling of pillar[5]arene-based bifunctional triflate **83** and boronic acids **84** with the use of chiral Sadphos ligand **L14** (Scheme 29a).[77] The significant steric hindrance and electronic properties of the aryl group in **L14** were reasoned to control the high reaction enantioselectivity (Scheme 30a).

Concurrently, a catalytic system comprising $Pd(TFA)_2$ and sterically chiral AKphos ligand **L15** was reported by Mazet, Leforestier and colleagues (Scheme 29b).[78] As with the previous approach, a high enantiomeric ratio was achieved with a broad spectrum of boronic acids. Stereodifferentiation of this transformation originates from both stabilizing secondary interactions and repulsive steric factors, as established computationally and experimentally (Scheme 30b).

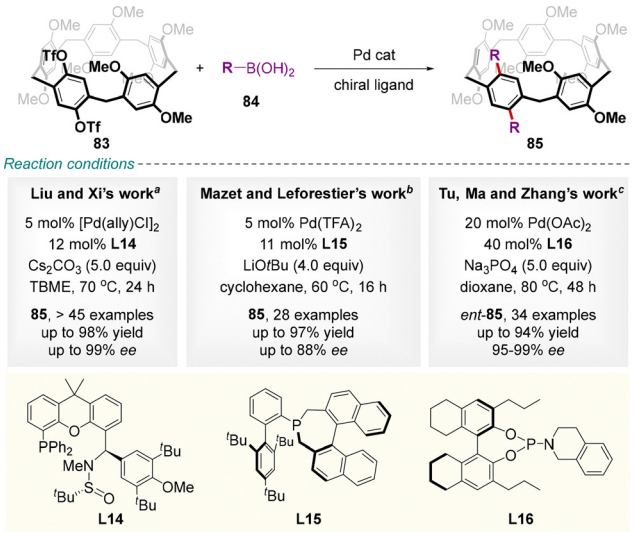

Scheme 29 Palladium-catalyzed asymmetric synthesis of inherently chiral pillar[5]arenes by DKR *via* Suzuki–Miyaura coupling.

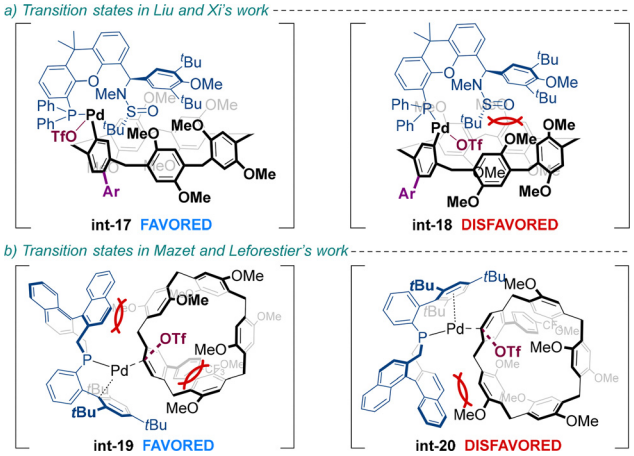

Scheme 30 Diastereomeric transition states in the Pd-catalyzed Suzuki–Miyaura coupling.

Soon after, a Pd(II)/chiral phosphoramidite **L16** catalytic system featuring higher enantioselectivity (95–99% ee) was provided by the Tu, Ma and Zhang's group (Scheme 29c).[79] By employing bulkier boronic acids, this protocol was successfully extended to the synthesis of configurationally stable, inherently chiral pillar[6]arenes. Mechanistic studies indicated that axial steric hindrance governs the conformational chirality-locking process in pillar[*n*]arenes. It is also noteworthy that in all three reactions above, the origin of stereoselectivity consistently identifies the second coupling as the enantio-determining step in the sequential double Suzuki–Miyaura coupling process.

3.3. Enantioselective copper-catalyzed alkyne–azide cycloaddition

Catalytic asymmetric Cu-catalyzed azide–alkyne cycloaddition (CuAAC) offers an efficient way for constructing structurally diverse centrally chiral triazoles and heterobiaryl atropisomers.[80,81]

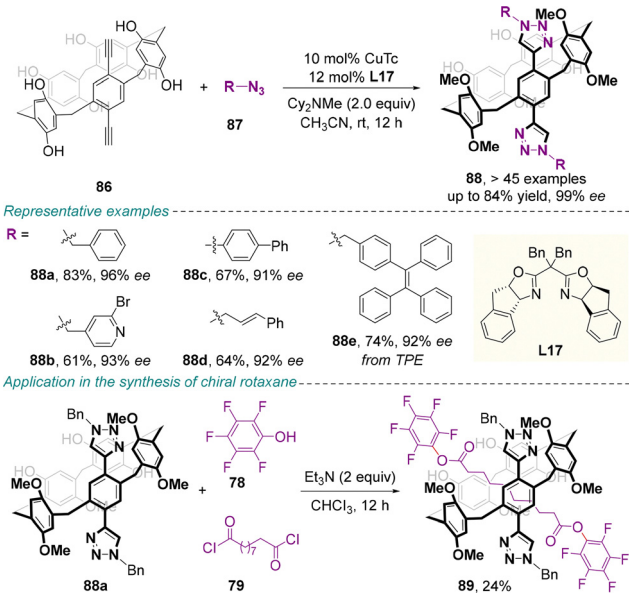

Scheme 31 Copper-catalyzed asymmetric synthesis of inherently chiral pillar[5]arenes by DKR *via* alkyne–azide cycloaddition.

However, this type of click reaction remained unexplored in producing inherently chiral scaffolds until recently. Based on the extended side-arm strategy, success with enantioselective CuAAC was achieved by Liu and co-workers using Cu(I) catalysis with chiral oxazoline-containing ligand **L17**, starting from 2-ethynyl-pillar[5]arene **86** (Scheme 31).[82]

The introduction of sterically hindered triazolyl groups afforded a diverse array of inherently chiral triazolyl-pillar[5]-arenes **88** in high yields with exceptional enantioselectivities. Ligand control studies confirmed that chiral induction occurs during the second catalytic step. The resulting products demonstrate high configurational stability; **88a**, for example, exhibits no racemization at 140 °C in xylene. Moreover, these enantiopure products enable the construction of chiral pillar[5]arene-based rotaxanes.

4. Enantioselective construction of saddle-shaped scaffolds

Beyond inherently chiral calix(het)arenes and pillar[*n*]arenes, rigid saddle-shaped medium-sized scaffolds, exemplified by tetraphenylene and its derivatives, represent another privileged class of persistent inherently chiral architectures. This unique chirality arises from their conformationally constrained structures, which impose high energy barriers to racemization. Such topologically defined frameworks underpin significant applications, ranging from chiral functional materials to bioactive molecules (*e.g.*, telenzepine).[27,28] However, the enantioselective synthesis of these saddle-shaped targets still remains a fundamental challenge. Modern catalytic asymmetric strategies now offer powerful and potentially transformative solutions to this long-standing problem.[17] This section surveys significant recent advances in this rapidly evolving field, organized by transition-metal catalysis and organocatalysis.

4.1. Transition-metal-catalyzed methods

4.1.1. Rhodium catalysis. In 2009, Shibata and co-workers pioneered innovative chiral rhodium-catalyzed consecutive inter- and intramolecular [2+2+2] cycloadditions of two phenylene-bridged 1,6,10-triynes **90**, affording saddle-shaped inherently chiral tetraphenylenes **91** with good to high yields and enantioselectivities (Scheme 32).[83]

This synthetic operation commences with the formation of rhodacyclopentadiene intermediate **int-21** from the 1,6-diyne moiety of the first triyne. Subsequently, the terminal alkyne moiety of the second triyne undergoes selective insertion into this intermediate to generate the primary cycloadduct **int-22** with axial chirality. Following this, oxidative coupling of the 1,6-diyne moiety in the second triyne forms the metallacycle **int-23**, and intramolecular coupling of the remaining terminal alkyne from the first triyne ultimately yields the eight-membered cycloadduct **91**.[84]

In 2016, the same group advanced the chemistry of enantioselective arene forming [2+2+2] cycloaddition further to derive enantioenriched saddle-shaped tribenzothiepins (Scheme 33).[85] This powerful and atom-economical approach provides efficient access for the synthesis of inherently chiral multisubstituted tribenzothiepins **94** and **96** from readily available diphenylsulfidetethered diynes **92** or 2-phenyl sulfanylbenzene-tethered diynes **95** using a rhodium catalyst in the presence of a chiral bidentate phosphorus ligand, respectively. Racemization measurements on optically pure tribenzothiepin **94a** revealed a racemization energy barrier of 29.1 kcal per mole, and the corresponding half-life of racemization at 20 °C was estimated to be 9.2 years.

As an extension of this strategy, Shibata and colleagues achieved the synthesis of the configurationally stable saddle-shaped cyclic polyarylenes **99** through the catalytic asymmetric

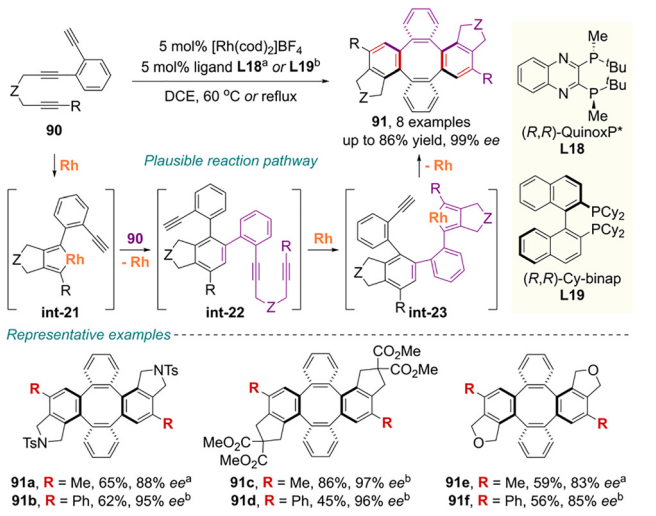

Scheme 32 Rhodium-catalyzed enantioselective synthesis of inherently chiral tetraphenylenes *via* consecutive cycloadditions.

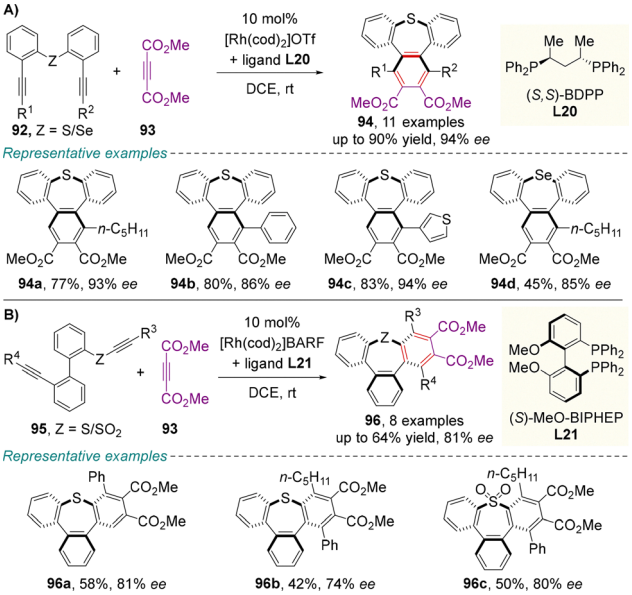

Scheme 33 Rhodium-catalyzed enantioselective synthesis of chiral saddle-shaped tribenzoheteropins *via* intermolecular cycloadditions.

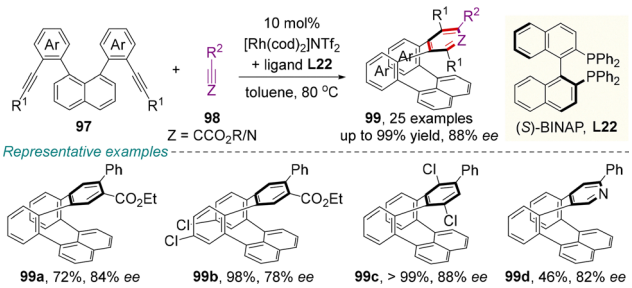

Scheme 34 Rhodium-catalyzed enantioselective synthesis of saddle-shaped cyclic polyarylenes *via* [2+2+2] cycloaddition.

intermolecular [2+2+2] cycloaddition of 1,8-naphthylene-based 1,10-diynes **97** with alkynoates **98** or aryl cyanides (Scheme 34).[86] The use of $[Rh(cod)_2]NTf_2$/(*S*)-BINAP afforded the corresponding inherently chiral cycloadducts **99** with good to high yields and enantioselectivities.

More recently, rhodium-catalyzed asymmetric synthesis of seven-membered saddle-shaped tribenzogermepins featuring inherent chirality has been demonstrated by Xiao and co-workers (Scheme 35).[87] In the presence of $[Rh(CH_2CH_2)_2Cl]_2$ with a chiral JosiPhos-based diphosphine ligand **L23**, a wide range of tribenzogermepins **101** were conveniently constructed in good to high yields with impressive enantioselectivities *via* dehydrogenative C(sp^2)–H germylation. These products are configurationally stable; for example, the theoretical half-life for racemization ($t_{1/2}$) of **101d** was determined to be 503 years at 25 °C.

4.1.2. Palladium catalysis. Besides the rhodium-catalyzed annulation, palladium-catalyzed cyclization reactions have also been devised for the enantioselective synthesis of saddle-shaped architectures.

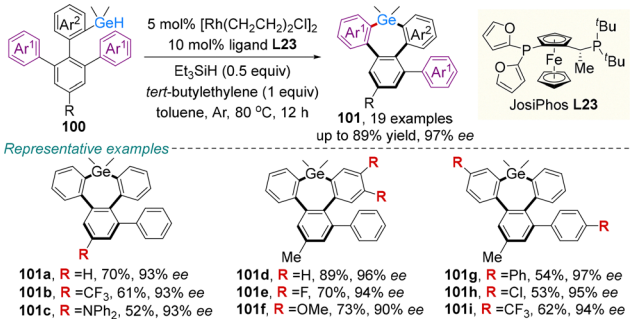

Scheme 35 Rhodium-catalyzed enantioselective synthesis of inherently chiral seven-membered tribenzogermepins *via* C–H germylation.

A prominent recent report by Zhu, Luo and colleagues documented the highly enantioselective three-component coupling reaction of various 2,2′-diisocyano-1,1′-biphenyl **102**, aryl iodide **103**, and carboxylate, promoted by a catalytic system comprising palladium(0) complex and Josiphos ligand **L24** (Scheme 36).[88] This reaction involves a sequence of oxidative addition of phenyl iodide **103**, migratory insertion of the first isocyano group of **102**, coordination of the second isocyano group to the Pd center, a second migratory insertion of the isocyano moiety and reductive elimination before migration of the Piv group to the *N*-atom of intermediate **int-27** to reveal the final saddle-shaped aza analog of tetraphenylene **104**. Stereochemical stability of this aza-bridged framework was typified by **104a**, for which the half-life was estimated to be 16 h at 100 °C. In addition, atropisomerically enriched compound **104a** could serve as a recyclable chiral acylating reagent for primary amines. This approach provides a sustainable route to

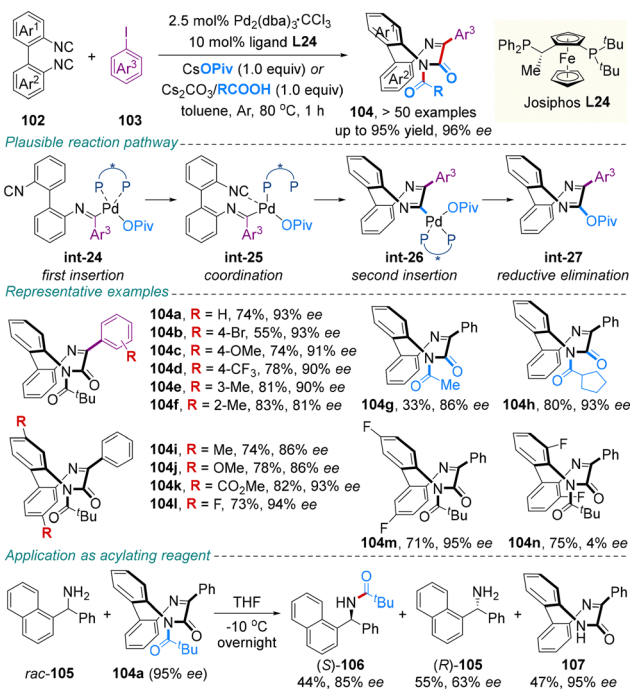

Scheme 36 Palladium-catalyzed enantioselective synthesis of a chiral saddle-shaped aza analog of tetraphenylene.

enantiomerically enriched amides, with promising applications in asymmetric synthesis and pharmaceutical chemistry.

In 2024, the same authors developed a palladium-catalyzed enantioselective carbene-based cross-coupling protocol using *N*-arylsulfonylhydrazone derivatives **108** and benzyl bromides **109** in the presence of *spiro*-phosphoramidite ligand **L25**, enabling the efficient construction of inherently chiral saddle-shaped tribenzoannulene derivatives **110** in high yields with exceptional enantioselectivities (Scheme 37, condition a).[89]

The proposed mechanism begins with oxidative addition of benzyl bromide to the Pd(0) catalyst to form Pd(II) complex **int-28**, which reacts with *in situ* generated diazo species to afford the palladium carbene intermediate **int-30**. Subsequent carbene migratory insertion, followed by β-hydride elimination, yields the insertion alkene products **110**. The β-hydride elimination step was identified as the stereocontrolling step of the entire reaction. The stability of inherent chirality of saddle-shaped **110** was substantial (**110a**, 31.7 kcal mol^{-1} at 140 °C). Notably, phosphine ligand **113**, derived from product **110e**, exhibited excellent catalytic performance in enantioselective Rh-catalyzed 1,4-addition and Pd-catalyzed Tsuji–Trost reactions, demonstrating its potential as a versatile platform for chiral phosphine ligand design. Concurrently, utilizing $Pd_2(dba)_3$ with chiral Feringa ligand **L26**, Liu and colleagues independently accomplished the same transformation with high yields and excellent enantioselectivities (Scheme 37, condition b).[90]

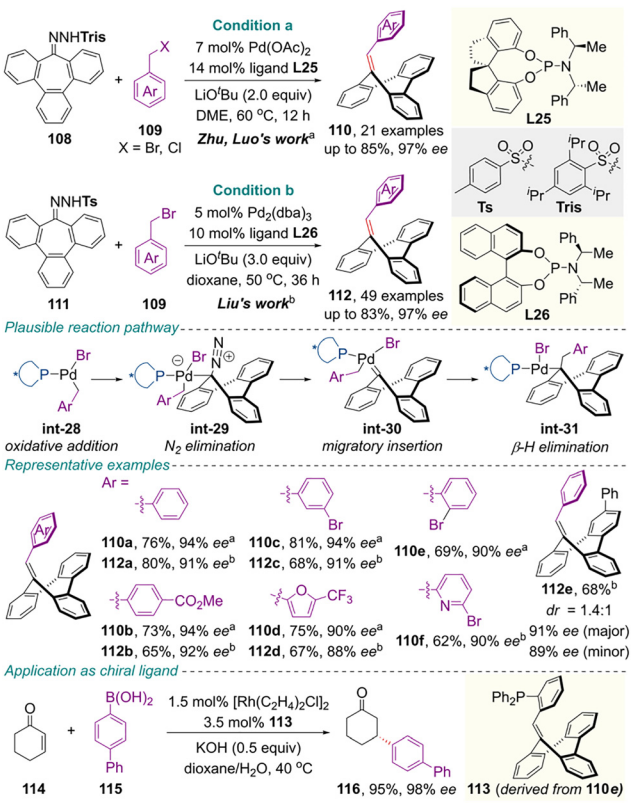

Scheme 37 Pd-catalyzed enantioselective synthesis of saddle-shaped tribenzoannulene derivatives *via* carbene-based cross-coupling.

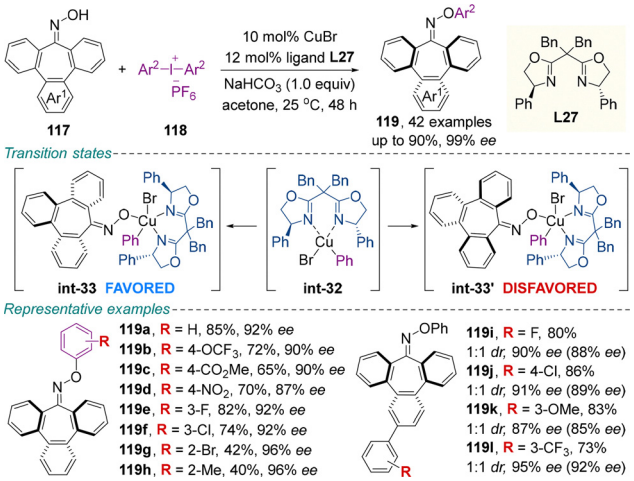

Scheme 38 Copper-catalyzed enantioselective synthesis of inherently chiral aryl oxime ethers *via* dynamic kinetic resolution.

4.1.3. Copper catalysis. Over the past few decades, diaryliodonium salts have received significant attention due to their importance in catalytic enantioselective transformations.[91] Very recently, Liu, Xu and co-workers reported CuBr/bisoxazoline catalyzed enantioselective *O*-arylation of tribenzotropone oximes **117** with diaryliodonium salts **118** for the synthesis of inherently chiral aryl oxime ethers **119** (Scheme 38).[92] This methodology smoothly produced various substituted enantioenriched tribenzocycloheptene oxime ethers in high to excellent enantioselectivities (up to 99% ee). Mechanistic investigations of plausible stereochemical models suggest that the C–H···π interactions between the phenyl moieties of ligand **L27** and oximes, as well as the C–H···Br interaction between the oxime and the bromine atom, should favor the formation of corresponding isomer **119**. Stereochemical stability studies of these chiral oxime ethers revealed that the rotational energy barrier of a model product **119a** was 28.9 kcal mol^{-1} at 80 °C, while the ee value dropped to 75% after 3.5 h in isopropanol at 80 °C.

4.2. Organocatalytic strategy

4.2.1. Chiral phosphoric acid catalysis. In addition to the copper-catalyzed C–O cross-coupling, chiral phosphoric acid catalyzed desymmetric condensation of tribenzotropones **120** and hydroxylamines **121** enables the enantioselective access to inherently chiral tribenzocycloheptene oxime ethers **122** (Scheme 39).[93] Under developed conditions, differing substitution environments of substrates **120** and **121** were well accommodated (up to 99% ee). On a 2.0 mmol scale, product **122f** was prepared in reasonable yield with excellent enantiopurity. Aside from hydroxylamines, tosylhydrazide and *N*-amino indole were equally suitable, albeit with moderate enantioselectivities.

In 2023, catalytic enantioselective cyclocondensation of easily available [1,1′-biphenyl]-2,2′-diamines **123** and substituted benzils **124** to construct saddle-shaped 6,7-diphenyldibenzo-[*e*,*g*][1,4]diazocines **125** portraying inherent chirality was contrived

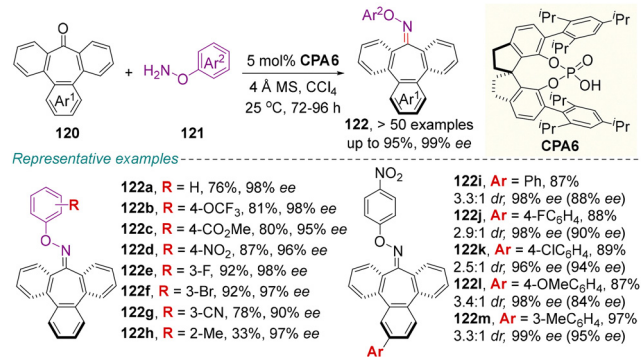

Scheme 39 CPA-catalyzed enantioselective synthesis of inherently chiral tribenzocycloheptene oxime ethers *via* a condensation reaction.

by Zhu, Luo and colleagues using H_8-BINOL-based chiral phosphoric acid catalysts (Scheme 40).[94] Precipitation and phase separation steps help increase the enantiomeric excess of the product. By changing the CPA catalyst **CPA7** to **CPA8**, an inversed product configuration was intriguingly acquired, although the two catalysts had the same configuration. The enantioselectivity was found to originate from the CPA-catalyzed dehydration step through non-covalent interactions, as elucidated by DFT calculations. Moreover, the configurationally stable diphenol derivative **126** served as a versatile synthetic platform, enabling the efficient construction of architecturally novel phosphoramidite ligands **127** and diphosphine ligands **128** while fully preserving enantiomeric excess. Preliminary catalytic tests showed that both ligands were

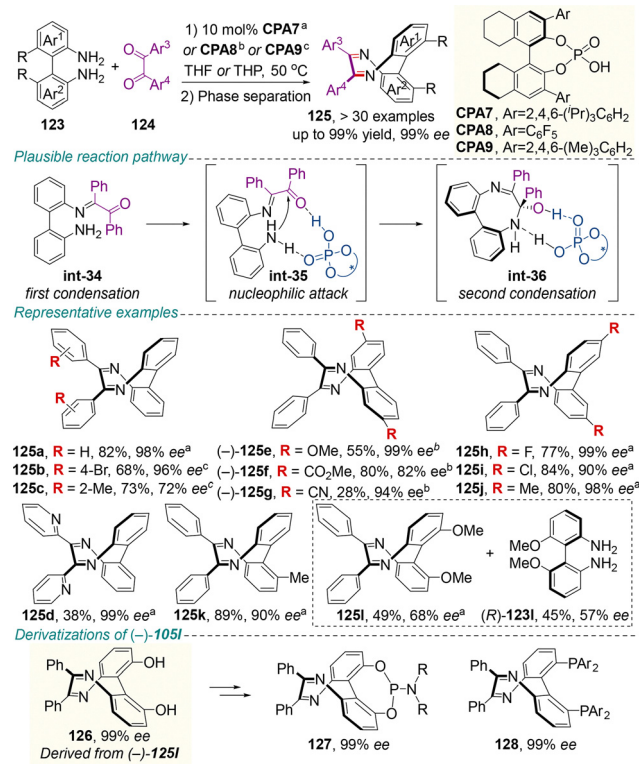

Scheme 40 CPA-catalyzed asymmetric synthesis of inherently chiral 6,7-diphenyldibenzo[*e*,*g*][1,4]diazocines *via* cyclocondensation.

effective in Pd- or Rh-catalyzed asymmetric reactions, providing enantioselectivities comparable to those from privileged scaffolds like BINOL and BINAP, highlighting the practical value of this methodology.

In related work, Yang and co-workers obtained good yields and an excellent enantioselective gateway to inherently chiral saddle-shaped dibenzo[*b*,*f*][1,5]diazocines **130** from asymmetric dimerization–cyclization of 2-acylbenzoisocyanates **129** enabled by chiral phosphoric acid **CPA10** (Scheme 41).[95] Notably, the incorporation of 2-acylaniline **131** as a co-catalyst enhanced the reaction efficiency, and the phase separation process improved enantioselectivity. The reaction initiates with the nucleophilic addition of **131** to **int-38**, followed by CO_2 release, generating the imine-type intermediate **int-40**. Following this, two plausible pathways were identified. The first pathway involves iterative addition, expulsion of CO_2, cyclization of **int-41** and elimination of aniline **131** with central-to-inherent chirality conversion of intermediate **int-42** to reveal the final product. Alternatively, the second pathway proceeds through CPA-guided stereoselective intramolecular condensation of **int-40**, followed by dehydration to generate the inherently chiral scaffold **130**.

In the same year, the same research group reported the CPA-catalyzed enantioselective synthesis of saddle-shaped inherently chiral 9,10-dihydrotribenzoazocines through two alternative methods: KR and DKR (Schemes 42 and 43).[96] In the KR pathway, using BINOL-derived catalyst **CPA5**, the intermolecular electrophilic amination proceeds with excellent selectivities (*s*-factors up to >1000). Racemization studies on optically pure (–)-**132a** revealed a racemization energy barrier of 27.33 kcal mol^{-1}, which suggested decent stereochemical stability of this scaffold. In the process of DKR, using SPINOL-derived **CPA11** as the catalyst in combination with Hantzsch ester **136** as

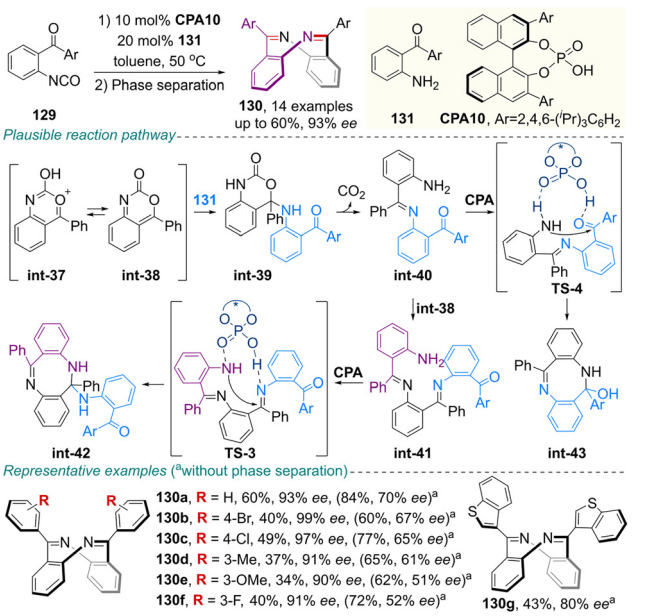

Scheme 41 CPA-catalyzed asymmetric synthesis of inherently chiral dibenzo[*b*,*f*][1,5]diazocines *via* dimerization of 2-acylbenzoisocyanates.

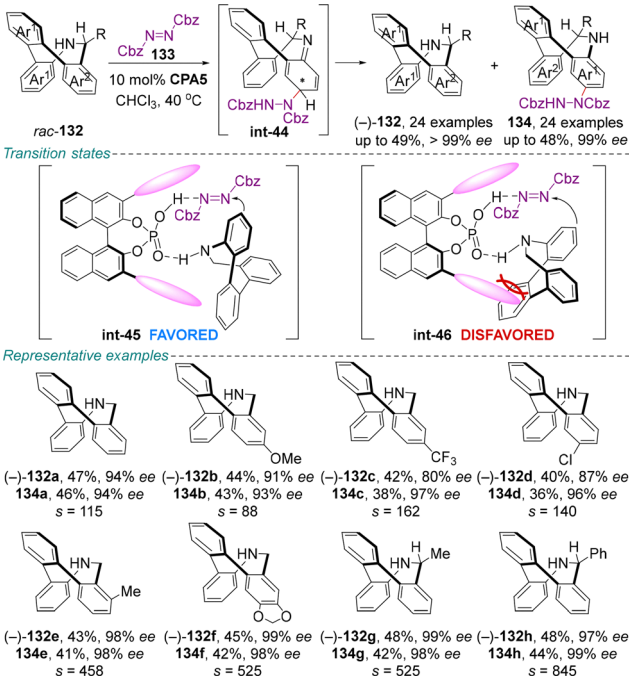

Scheme 42 CPA-catalyzed asymmetric synthesis of inherently chiral 9,10-dihydrotribenzoazocines *via* kinetic resolution.

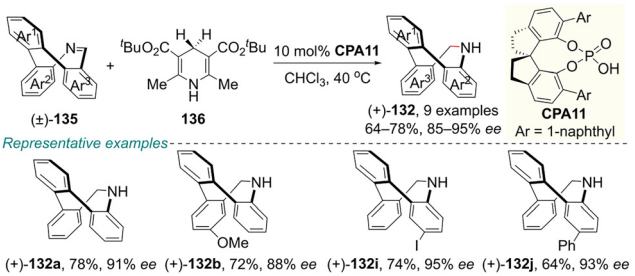

Scheme 43 CPA-catalyzed asymmetric synthesis of inherently chiral 9,10-dihydrotribenzoazocines *via* dynamic kinetic resolution.

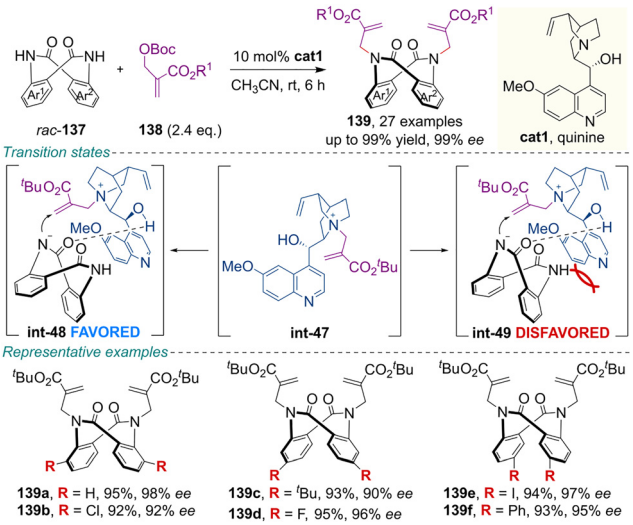

Scheme 44 Quinine-catalyzed enantioselective synthesis of chiral tub-shaped dianthranilides *via* dynamic kinetic resolution.

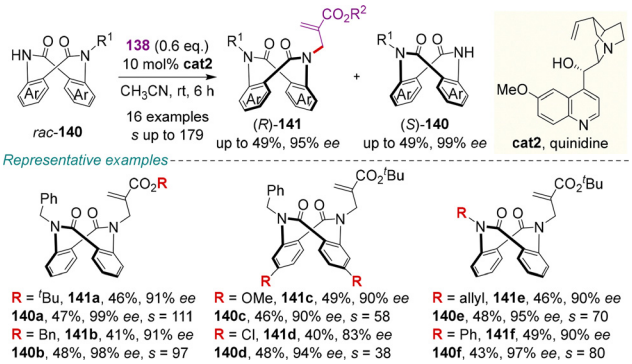

Scheme 45 Quinidine-catalyzed enantioselective synthesis of chiral tub-shaped dianthranilides *via* kinetic resolution.

the hydrogen source, asymmetric transfer hydrogenation of configurationally labile imine-type azaheterocycles **135** delivered 9,10-dihydrotribenzoazocines (+)-**132a** with good yields and high enantioselectivities.

4.2.2. Chiral cinchona alkaloid catalysis. In 2024, Mei, Huang and colleagues depicted the asymmetric cinchona alkaloid-catalyzed allylic alkylation of dianthranilides, providing a straightforward access to the optically active tub-shaped eight-membered cyclic dilactams (Schemes 44 and 45).[97] Using quinine **cat1** as the catalyst and Morita–Baylis–Hillman (MBH) adducts **138** as the alkylation reagent, the corresponding dialkylated products **139** were obtained efficiently through a DKR pathway with excellent yields and enantioselectivities. The first *N*-alkylation was suggested to be the DKR and enantio-determining step. In the case of mono-substituted racemic dianthranilides rac-**140**, the reaction proceeded in the presence of quinidine **cat2** *via* a KR process, affording the enantioenriched alkylated products (*R*)-**141** along with the enantioenriched starting materials (*S*)-**140**. Notably, this KR protocol was successfully applied to the enantioselective total synthesis of enantioenriched Eupolyphagin. Furthermore, the resulting products displayed significant and broad-spectrum anticancer activity, with **141d** showing high potency against A2780 cells (IC_{50} = 10.58 μM).

Recently, Yan, Liu and co-workers approached the highly chemo-, diastereo-, and enantioselective synthesis of novel rigid eight-membered *O*-heterocycles **144** and **146** possessing inherent chirality through a cross-[4+4] cycloaddition reaction, by harnessing the synthetic versatility of quinone methides (QMs) (Scheme 46).[98] Mechanistically, the quinidine-derived catalyst **cat3** enantioselectively processes the tautomerization of 2-alkynylnaphthol **142** to give axially chiral vinylidene *ortho*-quinone methide (VQM) intermediate **int-50** on which nucleophilic addition of *ortho*-quinone methide (*o*-QM) **143** proceeds to give **144**. Critically, the inherent chirality of the product was relayed from the enantioenriched VQM intermediate **int-50**. Apart from *o*-QMs **143**, *ortho*-hydroxyphenyl substituted *para*-quinone methides (*p*-QMs) **145** also react well for this transformation. DFT calculations confirmed the high stereochemical

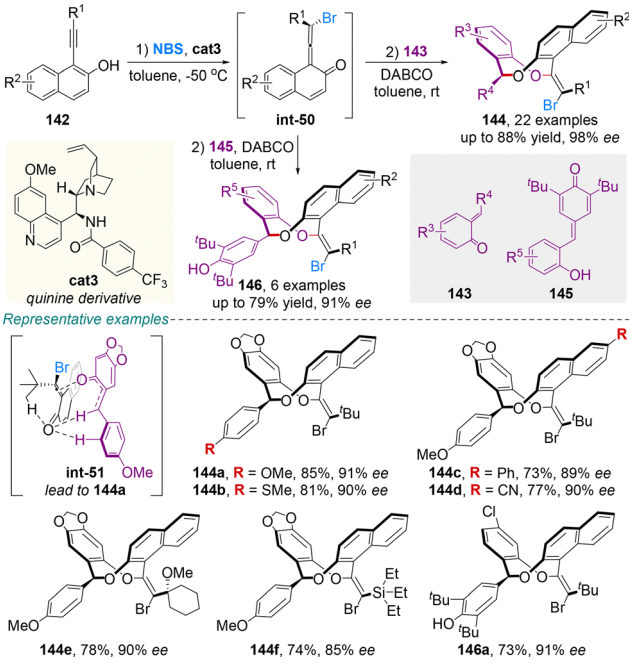

Scheme 46 Quinine-catalyzed enantioselective synthesis of chiral eight-membered *O*-heterocycles *via* cross-[4+4] cycloaddition.

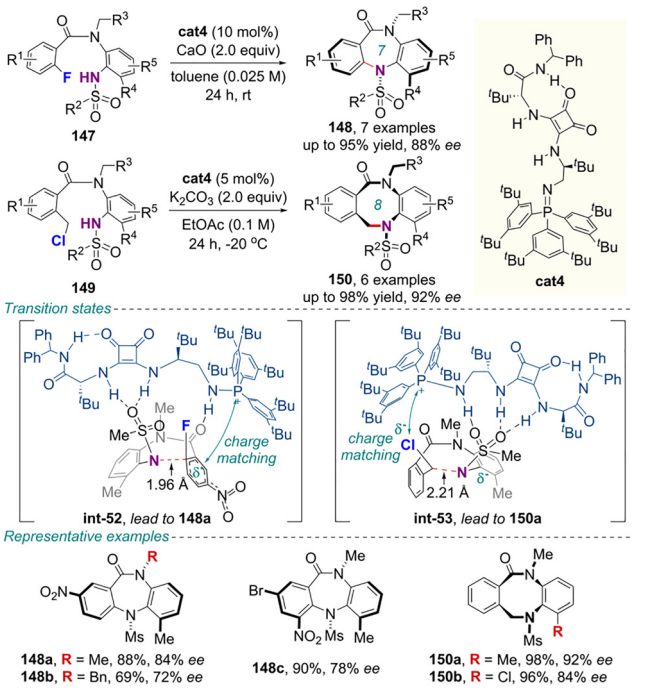

Scheme 47 Bifunctional iminophosphorane-catalyzed enantioselective synthesis of chiral seven- and eight-membered rings.

stability of these *O*-heterocycles ($\Delta G^{\ddagger}_{rac}$ = 48.2 kcal mol^{-1} for compound **144a**), with rigidity primarily arising from the bulky alkenes.

4.2.3. Chiral bifunctional iminophosphorane catalysis. More recently, Miller and colleagues pioneered an innovative chiral bifunctional iminophosphorane-catalyzed strategy leveraging substrate preorganization to achieve enantiocontrolled cyclization of inherently chiral medium-sized heterocycles (Scheme 47).[99]

The identical catalyst **cat4** facilitated the formation of seven- and eight-membered rings *via* two distinct mechanistic paradigms. The rotational barrier of model products **148a** and **150a** was determined to be >36 kcal mol^{-1} ($t_{1/2}$ > 900 000 years at 25 °C) and 27.5 kcal mol^{-1} ($t_{1/2}$ ≈ 200 days at 25 °C), respectively, confirming their configurational stability. Computational studies demonstrated that hydrogen-bonding interactions and minimization of substrate–catalyst dipole moments govern transition state assembly, whereas attractive dispersion forces substantially dictate the observed enantioselectivity and enantiodivergent behavior.

4.2.4. Chiral N-heterocyclic carbene catalysis. In 2024, using 1-(2-indolyl)naphthalen-2-ols **151** and α,β-alkynals **152** as substrates, Jiang, Wang, Hao and co-workers implemented formal high-order NHC-catalyzed [5+3] annulation to provide inherently chiral saddle-shaped eight-membered lactones **153** under exquisite enantiocontrol with chiral catalyst **NHC4** and Lewis acid Sc(OTf)$_3$ (Scheme 48).[100] Mechanistically, this reaction evolves *via* the formation of the Breslow intermediate **int-54** from ynal **152** in the presence of precatalyst **NHC4**. Hence, the intermediate **int-54** is oxidized by DQ and coordinated by Sc(OTf)$_3$ to afford the alkynyl acyl azolium-[*Sc*]-complex **int-55**.

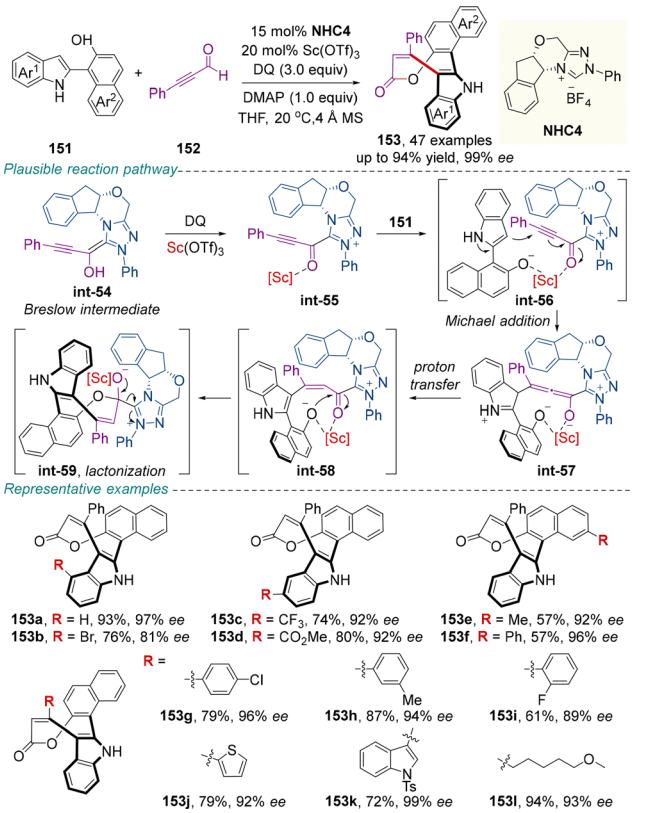

Scheme 48 NHC-catalyzed enantioselective synthesis of saddle-shaped eight-membered lactones *via* [5+3] annulation.

This complex subsequently coordinates with **151**, forming **int-56**, which undergoes a Michael addition to generate the allenolate

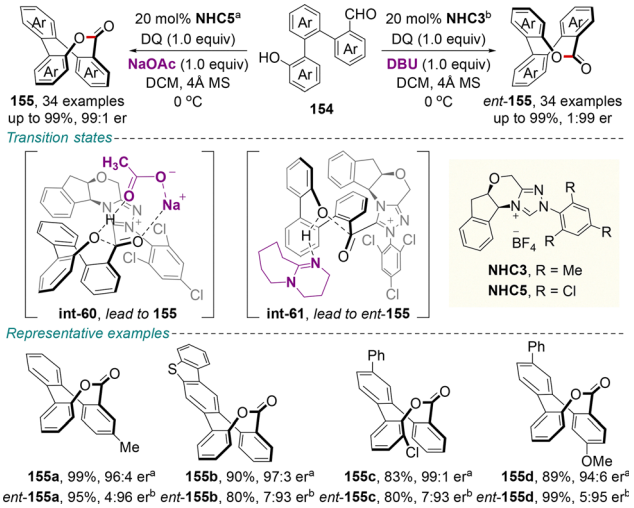

Scheme 49 NHC-catalyzed base-controlled enantiodivergent synthesis of 8-membered saddle-shaped lactones *via* intramolecular cyclization.

intermediate **int-57**. Proton transfer followed by lactonization and catalyst detachment ultimately delivers product **153**. Conformational stability of these oxocin-2-one scaffolds was testified with **153a** (racemization half-life of 5.5×10^4 h at 25 °C).

Recently, Yang, Zhang, Chi, and colleagues reported an efficient NHC-catalyzed, base-controlled enantiodivergent construction of inherently chiral, saddle-shaped 8-membered lactones from triaryl aldehydes **154** *via* intramolecular cyclization (Scheme 49).[101] Employing NHC catalysts sharing an identical chiral scaffold (**NHC3** or **NHC5**), but with different achiral bases, afforded both enantiomers of the lactones in high to excellent yields (up to 99%) with good to excellent enantioselectivities (up to 99 : 1 er for **155** and 1 : 99 er for ent-**155**). DFT studies revealed that this enantiodivergence stems from base-dependent noncovalent interactions governing the enantiodetermining transition state of the key acyl azolium intermediate. Notably, several enantiopure lactones exhibited potent antibacterial activity against plant pathogens, underscoring their potential for agricultural applications.

5. Enantioselective construction of rotaxanes

Mechanically interlocked molecules (MIMs), such as chiral rotaxanes and catenanes, can exhibit mechanical chirality (also referred to as inherent chirality) even when all covalent subcomponents are achiral.[18–20] This chirality originates from the relative spatial orientation enforced by the mechanical bond between the interlocked components, such as a ring and an axle, each possessing structural dissymmetry. In rotaxanes, mechanical chirality can arise from the symmetry breaking of achiral subunits due to conformational restrictions imposed by the mechanical bond, or through the introduction of steric hindrance to limit relative motion between the axle and the macrocycle. In catenanes, chirality can emerge when the two rings are traversed in a specific directional sequence, or when

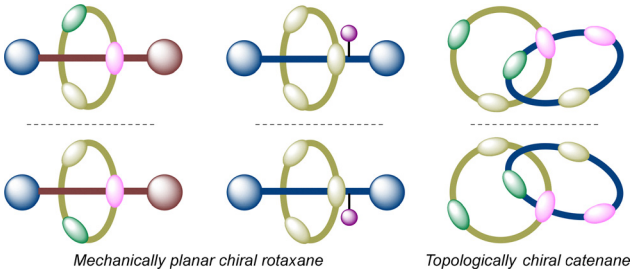

Fig. 2 Schematic presentation of a mechanically planar chiral rotaxane and topologically chiral catenane.

the macrocyclic faces are distinguishable (Fig. 2).[102–106] Despite holding considerable promise for applications spanning chiral sensing, supramolecular catalysis, and molecular machinery, the asymmetric synthesis of such architectures faces substantial challenges stemming from their conformational flexibility and noncovalent nature of mechanical bonds.

5.1. Dynamic kinetic resolution

In 2007, Takata and colleagues pioneered the catalytic enantioselective synthesis of inherently chiral rotaxanes **159** *via* a trialkylphosphane-catalyzed *O*-acylation of secondary ammonium salt **157** with bulky benzoic anhydride **158** (Scheme 50).[107] The enantioselectivity was governed by hydrogen bonding interactions between the phosphane groups in catalyst **cat5** and the amide moiety on the crown ether wheel **156**, with the rather low ee value (4.4%) suggesting that these interactions were insufficient to achieve effective facial discrimination of the crown ether.

In 2008, Leigh and colleagues reported the catalytic asymmetric synthesis of configurationally stable chiral benzyl ester rotaxanes **162** *via* DKR of enantiomeric hydroxyl-rotaxanes **160** (Scheme 51).[108] The two hydroxyl-rotaxane enantiomers, featuring four-point hydrogen bonding between a single fumaramide

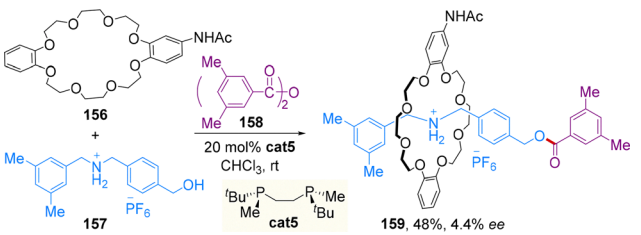

Scheme 50 Chiral trialkylphosphane-catalyzed asymmetric synthesis of inherently chiral rotaxanes *via* *O*-acylation.

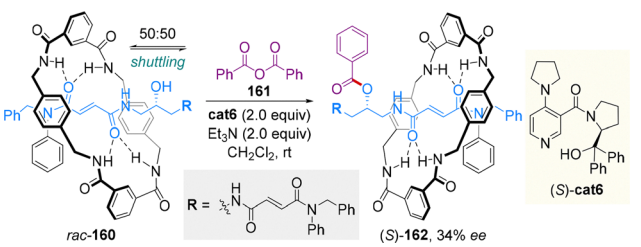

Scheme 51 Chiral DMAP derivative-catalyzed asymmetric synthesis of inherently chiral rotaxanes *via* dynamic kinetic resolution.

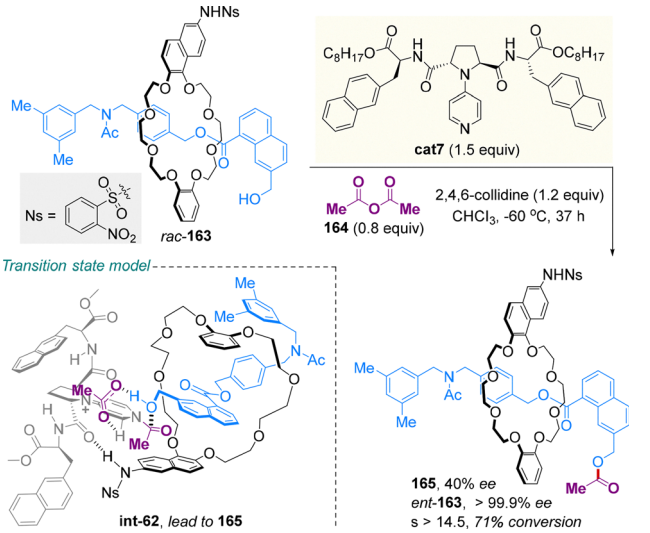

Scheme 52 Chiral 4-pyrrolidinopyridine-catalyzed enantioselective synthesis of mechanically planar chiral rotaxane *via* kinetic resolution.

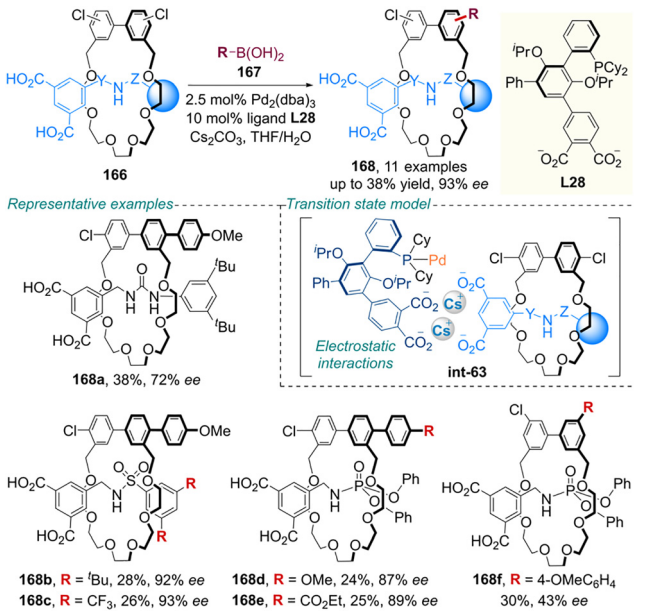

Scheme 53 Pd-catalyzed enantioselective synthesis of mechanically planar chiral rotaxane *via* desymmetrization.

moiety on the thread and the benzylic amide macrocycle, exist in equilibrium due to macrocycle shuttling. Employing a bulky chiral DMAP-derived catalyst (*S*)-**cat6** (2.0 equivalent) and benzoic anhydride **161**, asymmetric benzoylation installs a sterically demanding benzoyl group on the thread. This modification kinetically traps the macrocycle on one side, inhibiting shuttling and affording enantioenriched (*S*)-**162** with 34% ee.

5.2. Kinetic resolution

In 2021, Kawabata and colleagues reported the catalytic synthesis of enantiomerically enriched rotaxane **163** through kinetic resolution of the corresponding racemate (Scheme 52).[109] Treatment of racemic **163** with 0.8 equivalent amount of acetic anhydride **164** in the presence of 1.5 equivalent amount of catalyst **cat7** resulted in acylated rotaxane **165** after 37 h with 71% conversion. Analysis of the unreacted starting material ent-**163** revealed an enantiomeric excess >99.9% and a selectivity factor (s) > 14.5. Control experiments and ONIOM (our own *N*-layered integrated molecular orbital and molecular mechanics) calculations identified hydrogen-bonding interactions between the amide carbonyl group of catalyst **cat7** and the NsN–H moiety, along with general base catalysis by the proximal carboxylate anion adjacent to the reacting hydroxy group, as key factors enabling the effective remote asymmetric acylation.

5.3. Desymmetrization

In a significant advance, Zhu, Tian and co-workers developed a transformative catalyst-controlled desymmetrization strategy for the enantioselective synthesis of mechanically planar chiral (MPC) rotaxanes (Scheme 53).[110] This approach employs a Pd-catalyzed Suzuki–Miyaura coupling of prochiral, symmetrical bis(chloroaryl)macrocycle rotaxanes **166** with arylboronic acids **167**, utilizing the novel anionic chiral phosphine ligand **L28** to achieve high enantioselectivity (up to 93% ee). Of note, distal electrostatic interactions between the rotaxane and catalyst, mediated by carboxylate anions, predominantly govern precise stereocontrol, outweighing contributions from other types of non-covalent interactions. This strategy decouples chirality induction from mechanical bond formation, providing modular post-assembly access to MPC architectures and establishing the ionic ligand design as a robust paradigm for stereochemical manipulation in mechanically interlocked molecules.

6. Enantioselective construction of prism-like cages

In recent years, chiral peptide-mimic phosphonium salt (PPS) catalysis has emerged as a powerful and versatile strategy for accessing diverse enantiomerically enriched molecules.[111] In this realm, the first phosphonium-containing foldamer-catalyzed asymmetric synthesis of inherently chiral prism-like cages was realized by Wang and colleagues in 2024 *via* S_NAr desymmetrization (Scheme 54).[112] Employing a mild cationic foldamer catalysis system, a wide range of stereochemically rich, high-value prism-like cages **171** were prepared in good-to-high yields with high-to-excellent enantioselectivities across various aryl alcohol and thiol nucleophiles. From a mechanistic standpoint, the dual phosphonium centers of catalyst **PPS-1** would bind naphtholate anions through ion pairing, while N–H and benzyl C–H hydrogen-bonding sites within the peptide core would provide complementary non-covalent interactions. This synergistic ion-pairing/hydrogen-bonding network generates a chiral pocket that directs the stereoselective nucleophilic substitution of the chloride group in prochiral cage **169** by naphthol (*via* key intermediate **int-64**), enabling highly effective stereocontrol. Additionally, an enantiomer-selective (*M*-selective) kinetic resolution cycle involving intermediate **int-65** further

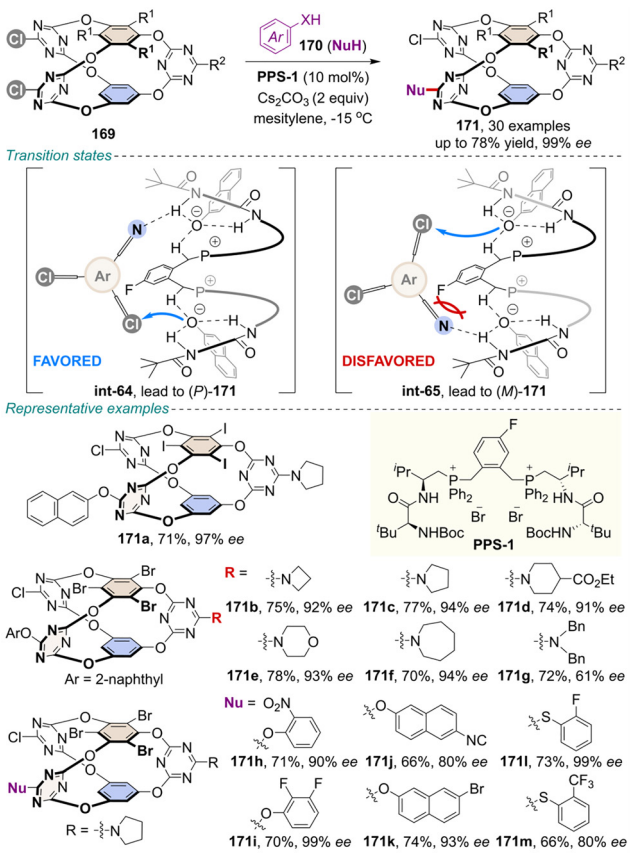

Scheme 54 Cationic foldamer-catalyzed enantioselective synthesis of inherently chiral cages *via* desymmetrization.

enhanced the enantioselectivity. Notably, the versatility of these stereogenic-at-cage building blocks was further highlighted by their application in the late-stage diversification of drug molecule skeletons.

7. Summary and outlook

Inherently chiral scaffolds constitute a structurally unique class of building blocks that are increasingly encountered in modern functional materials, medicinal chemistry, supramolecular catalysts, molecular recognition and self-assembly. Driven by persistent demand, significant efforts have been focused on the development of novel enantioselective synthetic strategies. In line with advances regarding enantioselective catalysis, methodologies have evolved from chiral separation techniques and stoichiometric chiral auxiliary-based approaches toward efficient catalytic protocols. Consequently, the catalytic asymmetric synthesis of inherently chiral scaffolds has undergone remarkable development, emerging as one of the rapidly evolving frontiers in synthetic chemistry.

Numerous efficient catalytic strategies, stemming from biocatalysis, transition-metal catalysis and organocatalysis, have been established, enabling access to diverse, value-added, and previously inaccessible enantiomerically pure inherently chiral architectures. These include heteracalix[4](het)arenes, rigid saddle-shaped medium-sized rings, and prism-like cages. Such progress offers valuable insights into designing novel catalytic asymmetric systems, expanding structural diversity and functional utility. Nevertheless, this field remains in its nascent stage. Moving forward, innovative research focusing on the following suggested directions holds considerable promise for accelerating the exploration of inherently chiral scaffolds in both academia and industry.

Firstly, practical access to potentially useful inherently chiral frameworks is often hampered by the limited substrate scope of contemporary synthetic methods. The vast majority of transformations rely on highly reactive, specifically designed precursors, constraining the accessible range of functionalized chiral scaffolds. Furthermore, catalytic asymmetric syntheses have been successfully developed for only a select few classes of inherently chiral systems to date, notably calix[4]arenes, seven- and eight-membered saddle-shaped scaffolds, mechanically interlocked rotaxanes, and prism-like cages. In contrast, significant synthetic challenges remain for other important classes, including calix[*n*]arenes (*n* = 3, 5, and 6),[67,113] additional rigid saddle-shaped medium-sized rings, mechanically interlocked catenanes and knots,[19,114,115] and other shape-persistent molecular cages. Expanding into these underrepresented architectures is imperative for exploring uncharted chemical space. Secondly, while inherent chirality arises from the overall spatial arrangement and intrinsic geometry of the entire molecular framework, it can often be generated through the enantioselective transformation of specific local regions. Consequently, established general catalytic enantioselective strategies that have been successful toward controlling classical chiral elements (central, axial,[116–118] planar,[119,120] and helical chirality[121]) may provide a valuable foundation for designing novel catalytic asymmetric syntheses of complex inherently chiral scaffolds. Building upon these proven methodologies will not only facilitate access to such unique architectures but may also reveal novel stereocontrol mechanisms. Finally, leveraging the power of computational and data-driven tools, such as artificial intelligence,[122] machine learning,[123] and advanced computational modeling, allows us to identify key factors governing conformational stability and characterizing rotational energy barriers in inherently chiral scaffolds. Such efforts may enable quantitative mapping of structure–chirality relationships, thus providing conceptual frameworks to guide the rational design of novel chemical transformations.

By systematically summarizing and discussing the advancements in this rapidly evolving field, this overview aims to inspire the development of conceptually novel catalytic strategies. The methodologies highlighted herein thus provide a fertile foundation for future innovation. Looking ahead, the pursuit of more efficient and truly versatile enantioselective catalytic methods is promising. By addressing current limitations, the field is poised to unlock access to hitherto unseen inherently chiral scaffolds. The development of such novel architectures and chemical space holds significant potential for applications in areas including medicinal chemistry, advanced functional materials, asymmetric synthesis, and molecular recognition and assembly.

Conflicts of interest

There are no conflicts to declare.

Data availability

No primary research results, software or code have been included and no new data were generated or analyzed as part of this review.

Acknowledgements

The authors gratefully acknowledge the financial support provided by the Key Science and Technology Project of Henan Province [Grant No. 252102310415], the Cultivation Fund of Huanghuai University for National Scientific Research Project (XKPY-2023012), and the Seeking Truth Talent Project of Hangzhou Medical College.

Notes and references

1 K. Mislow, *Introduction to stereochemistry*, W. A. Benjamin Publisher, New York, 1965.
2 K. Mislow and M. Raban, *Top. Stereochem.*, 1967, **1**, 1–38.
3 K. Mislow and J. Siegel, *J. Am. Chem. Soc.*, 1984, **106**, 3319–3328.
4 K. Mislow, *Croat. Chem. Acta*, 1996, **69**, 485–511.
5 V. Böhmer, D. Kraft and M. Tabatabai, *J. Inclusion Phenom. Mol. Recognit. Chem.*, 1994, **19**, 17–39.
6 A. Dalla Cort, L. Mandolini, C. Pasquini and L. Schiaffino, *New J. Chem.*, 2004, **28**, 1198–1199.
7 A. Szumna, *Chem. Soc. Rev.*, 2010, **39**, 4274–4285.
8 Y. Zheng and J. Luo, *J. Incl. Phenom. Macro.*, 2011, **71**, 35–56.
9 G. E. Arnott, *Chem. – Eur. J.*, 2018, **24**, 1744–1754.
10 P. Lhoták, *RSC Adv.*, 2024, **14**, 23303–23321.
11 W. Qin and G. Cera, *Chem. Rec.*, 2025, e202400237.
12 P. J. Cragg and K. Sharma, *Chem. Soc. Rev.*, 2012, **41**, 597–607.
13 K. Kato, S. Fa and T. Ogoshi, *Angew. Chem., Int. Ed.*, 2023, **62**, e202308316.
14 T. Ogoshi, T. Yamagishi and Y. Nakamoto, *Chem. Rev.*, 2016, **116**, 7937–8002.
15 X. Zhou and W. Wang, *Chem. – Eur. J.*, 2025, **31**, e202501185.
16 J. Han, J. Chen, X. Li, X. Peng and H. N. C. Wong, *Synlett*, 2013, 2188–2198.
17 Y. Luo, S. Luo and Q. Zhu, *J. Org. Chem.*, 2025, **90**, 5307–5322.
18 E. M. G. Jamieson, F. Modicom and S. M. Goldup, *Chem. Soc. Rev.*, 2018, **47**, 5266–5311.
19 S. M. Goldup, *Acc. Chem. Res.*, 2024, **57**, 1696–1708.
20 H. Yang, H. Feng, J. Chen and L. Zhou, *Chem. – Eur. J.*, 2025, **31**, e202500898.
21 K. E. Jelfs, X. Wu, M. Schmidtmann, J. T. A. Jones, J. E. Warren, D. J. Adams and A. I. Cooper, *Angew. Chem., Int. Ed.*, 2011, **50**, 10653–10656.
22 Y. Chen, G. Wu, B. Chen, H. Qu, T. Jiao, Y. Li, C. Ge, C. Zhang, L. Liang, X. Zeng, X. Cao, Q. Wang and H. Li, *Angew. Chem., Int. Ed.*, 2021, **60**, 18815–18820.
23 T. M. Fukunaga, T. Katoa, K. Ikemoto and H. Isobe, *Proc. Natl. Acad. Sci. U. S. A.*, 2022, **119**, e2120160119.
24 C. V. Maftei, E. Fodor, P. G. Jones, M. H. Franz, C. M. Davidescu and I. Neda, *Pure Appl. Chem.*, 2015, **87**, 415–439.
25 G. Sachdeva, D. Vaya, C. M. Srivastava, A. Kumar, V. Rawat, M. Singh, M. Verma, P. Rawat and G. K. Rao, *Coord. Chem. Rev.*, 2022, **472**, 214791.
26 O. Santoro and C. Redshaw, *Coord. Chem. Rev.*, 2021, **448**, 214173.
27 P. Eveleigh, E. C. Hulme, C. Schudt and N. J. Birdsall, *Mol. Pharmacol.*, 1989, **35**, 477–483.
28 H. R. Chobanian, Y. Guo, P. Liu, T. J. Lanza, M. Chioda, L. Chang, T. M. Kelly, Y. Kan, O. Palyha, X. Guan, D. J. Marsh, J. M. Metzger, K. Raustad, S. Wang, A. M. Strack, J. N. Gorski, R. Miller, J. Pang, K. Lyons, J. Dragovic, J. G. Ning, W. A. Schafer, C. J. Welch, X. Gong, Y. Gao, V. Hornak, M. L. Reitman, R. P. Nargund and L. S. Lin, *Biorg. Med. Chem.*, 2012, **20**, 2845–2849.
29 M. Tang and X. Yang, *Eur. J. Org. Chem.*, 2023, e202300738.
30 J. K. Browne, M. A. McKervey, M. Pitarch, J. A. Russell and J. S. Millership, *Tetrahedron Lett.*, 1998, **39**, 1787–1790.
31 C. Lu, Q. Xu, J. Feng and R. Liu, *Angew. Chem., Int. Ed.*, 2023, **62**, e202216863.
32 J. Feng, L. Xi, C. Lu and R. Liu, *Chem. Soc. Rev.*, 2024, **53**, 9560–9581.
33 K. Ishibashi, H. Tsue, H. Takahashi and R. Tamura, *Tetrahedron: Asymmetry*, 2009, **20**, 375–380.
34 S. Tong, J. T. Li, D. D. Liang, Y. E. Zhang, Q. Y. Feng, X. Zhang, J. Zhu and M. X. Wang, *J. Am. Chem. Soc.*, 2020, **142**, 14432–14436.
35 G. Hedouin, F. Hazra, S. Gallou and S. Handa, *ACS Catal.*, 2022, **12**, 4918–4937.
36 Y. Jiang, S. Tong, J. Zhu and M. Wang, *Chem. Sci.*, 2024, **15**, 12517–12522.
37 Y. Z. Zhang, M. M. Xu, X. G. Si, J. L. Hou and Q. Cai, *J. Am. Chem. Soc.*, 2022, **144**, 22858–22864.
38 X. Zhang, S. Tong, J. P. Zhu and M. X. Wang, *Chem. Sci.*, 2023, **14**, 827–832.
39 Y. You, H. Cheng, X. Huang, P. Wang, H. Cong, H. Cheng and Q. Zhou, *ChemRxiv*, 2024, preprint, DOI: **10.26434/chemrxiv-2024-d2zh7-v2**.
40 Y. Yu, J. M. Yang and J. Rebek, *Chem.*, 2020, **6**, 1265–1274.
41 I. Martín-Torres, G. Ogalla, J. Yang, A. Rinaldi and A. M. Echavarren, *Angew. Chem., Int. Ed.*, 2021, **60**, 9339–9344.
42 M. Li, C. K. S. Ho, I. K. W. On, V. Gandon and Y. Zhu, *Chem*, 2024, **10**, 3323–3341.
43 G. Giovanardi, G. Scarica, V. Pirovano, A. Secchi and G. Cera, *Org. Biomol. Chem.*, 2023, **21**, 4072–4083.
44 Q. Yao and B. Shi, *Acc. Chem. Res.*, 2025, **58**, 971–990.

45 T. Li, Y. Zhang, C. Du, D. Yang, M. Song and J. Niu, *Nat. Commun.*, 2024, **15**, 7673.
46 P. Qian, G. Zhou, J. Hu, B. Wang, A. Jiang, T. Zhou, W. Yuan, Q. Yao, J. Chen, K. Kong and B. Shi, *Angew. Chem., Int. Ed.*, 2024, **63**, e202412459.
47 X. Chang, Q. Zhang and C. Guo, *Angew. Chem., Int. Ed.*, 2020, **59**, 12612–12622.
48 C. Ma, J. Guo, S. Xu and T. Mei, *Acc. Chem. Res.*, 2025, **58**, 399–414.
49 X. Jiang, C. Zou, W. Zhuang, R. Li, Y. Yang, C. Yang, X. Xu, L. Zhang, X. He, Y. Yao, X. Sun and W. (Walter) Hu, *Green Chem.*, 2025, **27**, 915–945.
50 L. Zhang, C. Yang, X. Wang, T. Yang, D. Yang, Y. Dou and J. Niu, *Green Chem.*, 2024, **26**, 10232–10239.
51 Y. Mao, Y. Zhang, S. Tong, J. Zhu and M. Wang, *Org. Lett.*, 2023, **25**, 3936–3940.
52 R. Maji, S. C. Mallojjala and S. E. Wheeler, *Chem. Soc. Rev.*, 2018, **47**, 1142–1158.
53 E. I. Jiménez, *Org. Biomol. Chem.*, 2023, **21**, 3477–3502.
54 I. O. Betinol, Y. Kuang, B. P. Mulley and J. P. Reid, *Chem. Rev.*, 2025, **125**, 4184–4286.
55 X. Li, Y. Cheng, X. Wang, S. Tong and M. Wang, *Chem. Sci.*, 2024, **15**, 3610–3615.
56 X. Li, Y. Cheng, R. Jian, S. Tong, Y. Xia and M. Wang, *Org. Lett.*, 2025, **27**, 4603–4608.
57 R. Ibragimova, Q. Lu, M. Wang, J. Zhu and S. Tong, *Chem. – Asian J.*, 2025, **20**, e202401621.
58 J. Clerigué, M. T. Ramos and J. C. Menéndez, *Org. Biomol. Chem.*, 2022, **20**, 1550–1581.
59 B. C. Lemos, E. V. Filho, R. G. Fiorot, F. Medici, S. J. Greco and M. Benaglia, *Eur. J. Org. Chem.*, 2022, e202101171.
60 W. Xie, J. Zhou, W. Liu, T. Qin and X. Yang, *Cell Rep. Phy. Sci.*, 2024, **5**, 101993.
61 Y. Jiang, Y. Tian, J. Feng, H. Zhang, L. Wang, W. Yang, X. Xu and R. Liu, *Angew. Chem., Int. Ed.*, 2024, **63**, e202407752.
62 S. Yu, M. Yuan, W. Xie, Z. Ye, T. Qin, N. Yu and X. Yang, *Angew. Chem., Int. Ed.*, 2024, **63**, e202410628.
63 M. Yuan, W. Xie, S. Yu, T. Liu and X. Yang, *Nat. Commun.*, 2025, **16**, 3943.
64 X. Zhang, D. Zhu, R. Cao, Y. Huo, T. Ding and Z. Chen, *Nat. Commun.*, 2024, **15**, 9929.
65 V. Dočekal, L. Lóška, A. Kurčina, I. Císařová and J. Veselý, *Nat. Commun.*, 2025, **16**, 4443.
66 H. Han, X. Wang, S. Tong, J. Zhu and M. Wang, *ACS Catal.*, 2025, **15**, 6018–6024.
67 Y. Inaba, J. Yang, Y. Kakibayashi, T. Yoneda, Y. Ide, Y. Hijikata, J. Pirillo, R. Saha, J. L. Sessler and Y. Inokuma, *Angew. Chem., Int. Ed.*, 2023, **62**, e202301460.
68 Q. Lu, X. Wang, S. Tong, J. Zhu and M. Wang, *ACS Catal.*, 2024, **14**, 5140–5146.
69 Z. Li, J. Zhang, W. Zhu, T. Wang, Y. Tang and J. Wang, *Chem. Sci.*, 2025, **16**, 11021–11026.
70 H. Zhu, Q. Li, B. Shi, H. Xing, Y. Sun and S. Lu, *J. Am. Chem. Soc.*, 2020, **142**, 17340–17345.
71 J. F. Chen, Q. X. Gao, L. Liu, P. Chen and T. B. Wei, *Chem. Sci.*, 2023, **14**, 987–993.
72 H. Zhu, L. Chen, B. Sun, M. Wang, H. Li, J. F. Stoddart and F. Huang, *Nat. Rev. Chem.*, 2023, **7**, 768–782.
73 K. Wada and T. Ogoshi, *Mater. Chem. Front.*, 2024, **8**, 1212–1229.
74 H. Liang, B. Hua, F. Xu, L. S. Gan, L. Shao and F. Huang, *J. Am. Chem. Soc.*, 2020, **142**, 19772–19778.
75 Y. Sun, L. Liu, L. Jiang, Y. Chen, H. Zhang, X. Xu and Y. Liu, *J. Am. Chem. Soc.*, 2023, **145**, 16711–16717.
76 X. Zhou, X. Zhang, Y. Song, X. Li, L. Bao, W. Xu, X. Wang, H. Yang and W. Wang, *Angew. Chem., Int. Ed.*, 2025, **64**, e202415190.
77 T. Luan, C. Sun, Y. Tian, Y. Jiang, L. Xi and R. Liu, *Nat. Commun.*, 2025, **16**, 2370.
78 A. Konter, J. Rostoll-Berenguer, C. Besnard, B. Leforestier and C. Mazet, *ACS Catal.*, 2025, **15**, 2607–2619.
79 Y. Zhang, Y. Jiang, Y. Zhang, H. Wang, Z. Wu, R. Li, Y. Ma and T. Tu, *Chin. Chem. Lett.*, 2025, **36**, 111201.
80 W. D. G. Brittain, B. R. Buckley and J. S. Fossey, *ACS Catal.*, 2016, **6**, 3629–3636.
81 C. Qin, C. Zhao, G. Chen and Y. Liu, *ACS Catal.*, 2023, **13**, 6301–6311.
82 W. Zhou, L. Xi, M. Zhang, H. Wang, M. An, J. Li and R. Liu, *Angew. Chem., Int. Ed.*, 2025, **64**, e202502381.
83 T. Shibata, T. Chiba, H. Hirashima, Y. Ueno and K. Endo, *Angew. Chem., Int. Ed.*, 2009, **48**, 8066–8069.
84 T. Shibata, T. Uchiyama, H. Hirashima and K. Endo, *Pure Appl. Chem.*, 2011, **83**, 597–605.
85 Y. Tahara, R. Matsubara, A. Mitake, T. Sato, K. S. Kanyiva and T. Shibata, *Angew. Chem., Int. Ed.*, 2016, **55**, 4552–4556.
86 T. Shibata, M. Nakada, K. Senda and M. Ito, *Chem. – Eur. J.*, 2025, **31**, e202501193.
87 C. Qian, H. Yan, J. Li, Z. Zhang, Z. An and B. Xiao, *Org. Lett.*, 2025, **27**, 4118–4123.
88 Y. Luo, S. Cheng, Y. Peng, X. Wang, J. Li, C. Gan, S. Luo and Q. Zhu, *CCS Chem.*, 2022, **4**, 2897–2905.
89 X. Wang, C. Wang, Y. Luo, J. Li, C. Gan, S. Luo and Q. Zhu, *Chem. Catal.*, 2024, **4**, 100904.
90 H. Zhang, C. Lu, G. Cai, L. Xi, J. Feng and R. Liu, *Nat. Commun.*, 2024, **15**, 3353.
91 P. R. Singh, A. Banerjee and A. K. Simlandy, *ACS Catal.*, 2025, **15**, 3096–3115.
92 M. Zhang, H. Wang, H. Shan, L. Xi, C. Lu, X. Du, C. Sun, L. Xu and R. Liu, *Nat. Commun.*, 2025, **16**, 2505.
93 J. Li, X. Li, J. Feng, W. Yao, H. Zhang, C. Lu and R. Liu, *Angew. Chem., Int. Ed.*, 2024, **63**, e202319289.
94 Y. Luo, X. Wang, W. Hu, Y. Peng, C. Wang, T. Yu, S. Cheng, J. Li, Y. He, C. Gan, S. Luo and Q. Zhu, *CCS Chem.*, 2023, **5**, 982–993.
95 J. Zhou, M. Tang and X. Yang, *Chin. J. Chem.*, 2024, **42**, 1953–1959.
96 D. Zhang, J. Zhou, T. Qin and X. Yang, *Chem. Catal.*, 2024, **4**, 100827.
97 C. Guan, S. Zou, C. Luo, Z. Li, M. Huang, L. Huang, X. Xiao, D. Wei, M. Wang and G. Mei, *Nat. Commun.*, 2024, **15**, 4580.
98 D. Xu, G. Zhou, B. Liu, S. Jia, Y. Liu and H. Yan, *Angew. Chem., Int. Ed.*, 2025, **64**, e202416873.

99 N. Tampellini, B. Q. Mercado and S. J. Miller, *J. Am. Chem. Soc.*, 2025, **147**, 4624–4630.
100 S. Shi, C. Cui, L. Xu, J. Zhang, W. Hao, J. Wang and B. Jiang, *Nat. Commun.*, 2024, **15**, 8474.
101 L. Wei, Y. Chen, Q. Zhou, Z. Wei, T. Tu, S. Ren, Y. R. Chi, X. Zhang and X. Yang, *J. Am. Chem. Soc.*, 2025, **147**, 30747–30756.
102 A. W. Heard and S. M. Goldup, *ACS Cent. Sci.*, 2020, **6**, 117–128.
103 J. R. J. Maynard and S. M. Goldup, *Chem.*, 2020, **6**, 1914–1932.
104 J. P. Sauvage, *Angew. Chem., Int. Ed.*, 2017, **56**, 11080–11093.
105 J. F. Stoddart, *Angew. Chem., Int. Ed.*, 2017, **56**, 11094–11125.
106 D. A. Leigh, *Angew. Chem., Int. Ed.*, 2016, **55**, 14506–14508.
107 Y. Makita, N. Kihara, N. Nakakoji, T. Takata, S. Inagaki, C. Yamamoto and Y. Okamoto, *Chem. Lett.*, 2007, **36**, 162–163.
108 M. Alvarez-Pérez, S. M. Goldup, D. A. Leigh and A. M. Z. Slawin, *J. Am. Chem. Soc.*, 2008, **130**, 1836–1838.
109 A. Imayoshi, B. V. Lakshmi, Y. Ueda, T. Yoshimura, A. Matayoshi, T. Furuta and T. Kawabata, *Nat. Commun.*, 2021, **12**, 404.
110 M. Li, X. L. Chia, C. Tian and Y. Zhu, *Chem*, 2022, **8**, 2843–2855.
111 S. Fang, Z. Liu and T. Wang, *Angew. Chem., Int. Ed.*, 2023, **62**, e202307258.
112 S. Fang, Z. Bao, Z. Liu, Z. Wu, J. Tan, X. Wei, B. Li and T. Wang, *Angew. Chem., Int. Ed.*, 2024, **63**, e202411889.
113 G. Sachdeva, D. Vaya, C. M. Srivastava, A. Kumar, V. Rawat, M. Singh, M. Verma, P. Rawat and G. K. Rao, *Coord. Chem. Rev.*, 2022, **472**, 214791.
114 R. Jamagne, M. J. Power, Z. Zhang, G. Zango, B. Gibbera and D. A. Leigh, *Chem. Soc. Rev.*, 2024, **53**, 10216–10252.
115 L. Wu, M. Tang, L. Jiang, Y. Chen, L. Bian, J. Liu, S. Wang, Y. Liang and Z. Liu, *Nat. Synth.*, 2023, **2**, 17–25.
116 G. Liao and B. Shi, *Acc. Chem. Res.*, 2025, **58**, 1562–1579.
117 T. A. Schmidt, V. Hutskalova and C. Sparr, *Nat. Rev. Chem.*, 2024, **8**, 497–517.
118 S. Xiang, W. Ding, Y. Wang and B. Tan, *Nat. Catal.*, 2024, **7**, 483–498.
119 G. Yang and J. Wang, *Angew. Chem., Int. Ed.*, 2024, **63**, e202412805.
120 K. Zhu, L. Yang, Y. Yang, Y. Wu and F. Zhang, *Chin. Chem. Lett.*, 2025, **36**, 110678.
121 Y. Wang, Z. Wu and F. Shi, *Chem. Catal.*, 2022, **2**, 3077–3111.
122 A. M. Mroz, A. R. Basford, F. Hastedt, I. S. Jayasekera, I. Mosquera-Lois, R. Sedgwick, P. J. Ballester, J. D. Bocarsly, E. A. R. Chanona, M. L. Evans, J. M. Frost, A. M. Ganose, R. L. Greenaway, K. K. (Mimi) Hii, Y. Li, R. Misener, A. Walsh, D. Zhang and K. E. Jelfs, *Chem. Soc. Rev.*, 2025, **54**, 5433–5469.
123 J. Xia, Y. Zhang and B. Jiang, *Chem. Soc. Rev.*, 2025, **54**, 4790–4821.